Molecular Biology of the Cell
Vol. 21, 287–301, January 15, 2010

Identification of MYO18A as a Novel Interacting Partner of the PAK2/βPIX/GIT1 Complex and Its Potential Function in Modulating Epithelial Cell Migration

Rae-Mann Hsu,* Ming-Hung Tsai,* Ya-Ju Hsieh,† Ping-Chiang Lyu,† and Jau-Song Yu*‡§

*Graduate Institute of Biomedical Sciences, ‡Department of Cell and Molecular Biology and §Proteomics Core Laboratory, College of Medicine, Chang Gung University, Tao-Yuan, Taiwan, Republic of China; and †Department of Life Sciences and Institute of Bioinformatics and Structural Biology, National Tsing Hua University, Hsinchu, Taiwan, Republic of China

Submitted March 20, 2009; Revised October 15, 2009; Accepted November 6, 2009
Monitoring Editor: Jonathan Chernoff

The p21-activated kinase (PAK) 2 is known to be involved in numerous biological functions, including the regulation of actin reorganization and cell motility. To better understand the mechanisms underlying this regulation, we herein used a proteomic approach to identify PAK2-interacting proteins in human epidermoid carcinoma A431 cells. We found that MYO18A, an emerging member of the myosin superfamily, is a novel PAK2 binding partner. Using a siRNA knockdown strategy and in vitro binding assay, we discovered that MYO18A binds to PAK2 through the βPIX/GIT1 complex. Under normal conditions, MYO18A and PAK2 colocalized in lamellipodia and membrane ruffles. Interestingly, knockdown of MYO18A in cells did not prevent formation of the PAK2/βPIX/GIT1 complex, but rather apparently changed its localization to focal adhesions. Moreover, MYO18A-depleted cells showed dramatic changes in morphology and actin stress fiber and membrane ruffle formation and displayed increases in the number and size of focal adhesions. Migration assays revealed that MYO18A-depleted cells had decreased cell motility, and reexpression of MYO18A restored their migration ability. Collectively, our findings indicate that MYO18A is a novel binding partner of the PAK2/βPIX/GIT1 complex and suggest that MYO18A may play an important role in regulating epithelial cell migration via affecting multiple cell machineries.

INTRODUCTION

The p21-activated kinases (PAKs) comprise an evolutionarily conserved family of serine/threonine kinases that are important for a variety of cellular functions. The PAKs were the first identified binding partners of GTP-bound forms of p21 GTPase Rac1 or Cdc42; this binding triggers a cascade of autophosphorylation events that culminate in full phosphorylation and kinase activation (Manser *et al.*, 1994; Bagrodia *et al.*, 1995; Knaus *et al.*, 1995; Martin *et al.*, 1995). The PAK family currently consists of six members, Pak1 through Pak6 (Manser *et al.*, 1994; Abo *et al.*, 1998; Sells *et al.*, 1999; Dan *et al.*, 2002; Lee *et al.*, 2002), all of which have similar structures containing an N-terminal regulatory domain and a C-terminal kinase domain. Based on structural and architectural similarities, the PAK family members may be divided into two groups: conventional group I, which includes PAK1, PAK2, and PAK3, and unconventional group II, which includes PAK4, PAK5, and PAK6 (Jaffer and Chernoff, 2002). Although we are only beginning to understand the structures and regulations of group II PAKs, the biological roles and regulations of the group I PAKs, especially those of PAK1, have been widely studied.

The function of PAK family members is regulated via changes in its catalytic activity or through regulation of the binding of PAK-interacting proteins. Numerous studies have reported stimulation of PAKs by stimuli such as growth factors, cytokines, and wounding (Royal *et al.*, 2000; Beeser *et al.*, 2005). Activation of PAKs plays a critical role not only in cell morphogenesis, mitosis, survival, neurogenesis, and cancer metastasis, but also in regulation of the cytoskeleton and cell motility (Bokoch, 2003; Coniglio *et al.*, 2008). Unique among the PAKs, PAK2 is cleaved by caspase-3 during apoptosis. The cleaved C-terminal domain of PAK2 appears to become catalytically activated and induces striking proapoptotic alterations in cellular and nuclear morphology (Lee *et al.*, 1997; Rudel and Bokoch, 1997; Walter *et al.*, 1998).

Of all the PAK-interacting proteins, the best studied are the guanine nucleotide exchange factor, PIX (PAK-interacting exchange factor), and its binding partner, GIT1 (G-protein–coupled receptor kinase-interactor 1), which appear to be crucial for many PAK functions. The first identified PAK-interacting proteins were αPIX and βPIX (Manser *et al.*, 1998; Manabe *et al.*, 2002). The PIX proteins were predicted to exhibit guanine nucleotide exchange factor (GEF) activity based on the presence of a conserved characteristic of Rho-

This article was published online ahead of print in *MBC in Press* (http://www.molbiolcell.org/cgi/doi/10.1091/mbc.E09–03–0232) on November 18, 2009.

Address correspondence to: Jau-Song Yu (yusong@mail.cgu.edu.tw).

Abbreviations used: GIT1, G-protein–coupled receptor kinase-interactor 1; GEF, guanine nucleotide exchange factor; GST, glutathione *S*-transferase; MALDI-TOF, matrix-assisted laser desorption/ionization-time of flight; MS, mass spectrometry; PAK2, p21-activated kinase 2; PIX, PAK-interacting exchange factor.

GTPase GEF proteins: a tandem DH/PH (Dbl homology/Pleckstrin homology) domain (Feng *et al.*, 2002). PIX proteins directly interact with a specific proline-rich domain in PAKs through a SH3 domain and thereafter colocalize to focal adhesions and cooperate in the formation of lamellipodia and membrane ruffles (Obermeier *et al.*, 1998, Koh *et al.*, 2001). Complexes of PAK and PIX have been associated with p95PKL (paxillin kinase linker; Turner *et al.*, 1999), CAT (cool-associated, tyrosine-phosphorylated; Bagrodia *et al.*, 1999), and GIT1 (Manabe *et al.*, 2002); these associations allow PAK to coordinate cytoskeletal reorganization. PAK/βPIX/GIT complexes play important roles in cytoskeletal dynamics and cell motility, and the dynamic assembly and disassembly of the complexes is highly regulated. To date, numerous studies have shown that PAK/βPIX/GIT-containing complexes are targeted to focal contacts and are implicated in the dynamic regulation of these adhesion sites. However, the precise targeting mechanisms and functions of these proteins at focal contacts remain ambiguous (Zegers, 2008).

In the present study, we used a proteomic approach to identify MYO18A, a member of the myosin superfamily, as a novel PAK2-binding partner. Our biochemical and cell biology data show that MYO18A interacts with PAK2 through the βPIX/GIT1 complex and suggest its potentially important role in modulating membrane ruffle formation, focal adhesion turnover, actin filament reorganization, and migration ability of epithelial cells.

MATERIALS AND METHODS

Cell Culture and Transfection

Human epidermoid carcinoma A431 cells, HEK293 cells, and cervical cancer cells (HeLa) were cultured as previously described (Tsai *et al.*, 2005; Wu *et al.*, 2005). Cells were washed twice with cold PBS, collected and disrupted in appropriate amounts of lysis buffer (10 mM Tris-HCl, pH 7.4, 2 mM EDTA, 1 mM EGTA, 50 mM NaCl, 1% Triton X-100, 1 mM phenylmethylsulfonyl fluoride, 1 mM benzamidine, 0.5 μg/ml aprotinin, 50 mM NaF, 20 mM sodium pyrophosphate, and 0.2 mM sodium orthovanadate). Cell lysates were centrifuged at 15,000 × *g* for 20 min at 4°C, and the supernatants were used as the cell extracts for most experiments. Protein concentrations were measured with a BCA protein assay kit from Pierce (Rockford, IL). For siRNA transfection, cells were plated at a density of 1×10^5 cells per well in six-well plates for 4 h and then transfected using 20 nM of siRNA duplex with 1.3 μg/ml Lipofectamine 2000 (Invitrogen, Carlsbad, CA). Cells were transfected overnight, and fresh medium was added 24 h after transfection.

In-Gel Tryptic Digestion and Mass Spectrometric Analysis

In-gel tryptic digestion of silver-stained proteins and mass spectrometric analysis were carried out as previously described (Tsai *et al.*, 2005; Wu *et al.*, 2005). Matrix-assisted laser desorption/ionization-time of flight (MALDI-TOF) mass spectrometric analysis was performed on an Ultraflex MALDI-TOF/TOF mass spectrometer (Bruker Daltonik, Bremen, Germany).

Antibodies

Commercial antibodies against PAK2 (V19), GIT1, glutathione *S*-transferase (GST), His tag, Myc tag, MYO18A (N15), and tubulin were from Santa Cruz Biotechnology (Santa Cruz, CA). The anti-vinculin antibody was from Sigma (St. Louis, MO). The anti-βPIX antibody was from Transduction Laboratories (Lexington, KY). The anti-PAK2 (N17) antibody was produced in rabbits using a peptide corresponding to the N-terminal region of human and rabbit PAK2 (amino acids 1-17; MSDNGELEDKPPAPPVR), as described previously (Tang *et al.*, 1998; Chan *et al.*, 2000). The anti-MYO18A polyclonal antibodies were produced in rabbits using the C15 peptide corresponding to the C-terminal amino acids of the human MYO18A sequence (amino acids 2049-2054; CYLSDSTEAKLTETNA). The C15 peptide was synthesized by Kelowna International Scientific (Taipei, Taiwan). A cysteine residue was added to the NH_2-terminus of the C15 peptide to facilitate coupling to bovine serum albumin (BSA; as a carrier protein). The anti-C15 peptide antibodies were affinity-purified by Sepharose 4B (GE Healthcare, Little Chalfont, Buckinghamshire, United Kingdom) coupled with C15 peptide. After purification, anti-C15 peptide antibodies were concentrated and stored in 50% glycerol in PBS at −20°C.

Gel Filtration

A431 cells were grown to confluence in DMEM containing 10% serum. Cells were scraped into gel filtration buffer (0.05 M Tris, 0.15 M NaCl, and 1 mM EDTA), triturated, and centrifuged as described above. The lysate (1 mg protein) was further filtered through a 0.2-μm syringe filter and loaded onto a Superose 12 column (10/300 size, Amersham Biosciences, Sunnyvale, CA). The column was developed with gel filtration buffer at a flow rate of 0.2 ml/min at 4°C, and fractions were collected at 0.5 ml/tube. Molecular-weight standard proteins were run under the same conditions.

Plasmid Construction

PAK2 Clones. The full-length cDNA of human PAK2 (PAK2FL) was PCR amplified from cDNAs derived from A431 cells using specific primers (forward 5′-GAAGATCTTCATGTCTGATAACGGAGAA-3′; reverse 5′-GAAGATCTTCTTAACGGTTACTCTTCAT-3′). Purified PCR products were T/A cloned into the pGEM-T vector (Promega, Madison, WI). The PAK2FL cDNA was BglII digested from pGEM-T/PAK2FL and ligated to the pCMV-Myc vector (Clontech, Mountain View, CA). The cDNA corresponding to the PAK2 N-terminal regulatory domain (PAK2N, aa 1-212) was NcoI digested from GEM-T/PAK2FL, blunted with Klenow fragment, and then digested with BglII. The digested product (PAK2N cDNA) was subsequently ligated to pCMV-Myc vector that had been predigested with KpnI, blunted with Klenow fragment, and digested with BglII. The resulting plasmid was designated pCMV-Myc/PAK2N. The cDNA corresponding to the PAK2 kinase domain (PAK2KC, aa 213-524) was AflIII digested from pGEM-T/PAK2FL, blunted with Klenow fragment, and then digested with NotI. The digested product was then ligated to pCMV-Myc vector that had been predigested with EcoRI, blunted with Klenow fragment, and digested with NotI. To generate pET-15b/PAK2FL, the PAK2FL cDNA was SacII digested from pGEM-T/PAK2FL, blunted with Klenow fragment, and then digested with SmaI. The digested product was ligated to pET-15b (Novagen, Merck Bioscience, Darmstadt, Germany) vector that had been predigested with XhoI and blunted with Klenow fragment. PAK2 mutant that does not bind to PIX (PAK2-P185G/R186A; Renkema *et al.*, 2001) was generated by site-directed mutagenesis using a QuickChange site-directed mutagenesis kit (Stratagene, La Jolla, CA). pCMV-Myc/PAK2FL was used as a template, and the primer used for site-directed mutagenesis had the sequence 5′-GCTCCTCCCGTTATTGCCGG GGCACCGGATCATACGAAATC-3′, where the underlined bases represent the positions to be mutated. The DNA sequence of the resulting PAK2 mutant was confirmed by autosequencing.

MYO18A Clones. The MYO18A cDNA KIAA0216 clone hf00331s1 inserted in the KpnI and NotI site of pBluescript II SK (+) plasmid was kindly provided from the Kazusa DNA Research Institute (Japan). The MYO18A cDNA was subcloned into the pCMV-Myc vector. To prevent the inclusion of undesired coding sequences, primers (forward 5′-CGGAATTCCGATGTTTAACCTAATGAAGAAAGA-3′ and reverse 5′-TGGCCCTCGGGGCCC-3′) were designed to amplify the cDNA from the start codon of MYO18A to 841 base pairs. Purified PCR products were then subcloned into the pBluescript II SK (+)/KIAA0216 plasmid predigested with EcoRI and SfiI, to replace the original sequence. The full-length MYO18A (MYO18A-FL) cDNA was KpnI and NotI digested from the "new" pBluescript II SK (+)/KIAA0216 plasmid, blunted with Klenow fragment, and then ligated into the pCMV-Myc vector to generate pCMV-Myc/MYO18A-FL. The MYO18A-FL cDNA was then subcloned into the pEGFP-C3 vector to generate pEGFP-C3/MYO18A-FL, which could express an EGFP-MYO18A fusion protein with an NH_2-terminal EGFP tag. pCMV-Myc/MYO18A-N was generated from pCMV-Myc/MYO18A-FL by restriction enzyme digestion using SfiI and HindIII to remove unwanted sequences. The removed sequences were recovered, blunted with Klenow fragment, and ligated into the pCMV-Myc vector to generate pCMV-Myc/MYO18A-C. pCMV-Myc/MYO18A-C was then digested with NotI and SmaI and self-ligated to obtain pCMV-Myc/MYO18A-CA. MYO18A-CB was NotI and SmaI digested from pCMV-Myc/MYO18A-C and subcloned into the pCMV-Myc vector to generate pCMV-Myc/MYO18A-CB. MYO18A-CB-L was NotI and HinfI digested from pCMV-Myc/MYO18A-CB and subcloned into the pCMV-Myc vector to generate pCMV-Myc/MYO18A-CB-L. MYO18A-CB-S was HinfI and SmaI digested from pCMV-Myc/MYO18A-CB and subcloned into the pEGFP-C3 vector to generate pEGFP-C3/MYO18A-CB-S. For expression of the GST-MYO18A-CB fusion protein, MYO18A-CB was SmaI and NotI digested from pCMV-Myc/MYO18A-C, treated with Klenow fragment, and then subcloned into a pGEX-3X vector that had been predigested with SmaI, to generate pGEX-3X/MYO18A-CB. For the expression of his-MYO18A-CB fusion protein, MYO18A-CB was PCR amplified from pCMV-Myc/MYO18A-CB using specific primers (forward 5′-CATATGGACCTGGCTCAGATAAATGATCTC-3′; reverse 5′-CTCGAGCTATGCGTTAGTCTCCGTCAGCTT-3′). Purified PCR products were then predigested with NdeI and XhoI and subcloned to the pET-15b vector (Novagen, Madison, WI).

Other Clones. Paxillin-DsRed2, pXJ40-GST-GIT1, and pGEX-6P-bPIX are kindly gifts from Dr. Donna Webb (Vanderbilt University, Tennessee), Dr. Edward Manser (Institute of Molecular and Cell Biology, National University

of Singapore), and Dr. Peter L. Hordijk (Department Molecular Cell Biology, Sanquin Research, the Netherlands), respectively. To generate inactive His-tagged caspase 3, full-length human caspase-3 gene was PCR amplified from cDNAs derived from A431 cells using specific primers (forward 5′-GGAATTCCATATGGAGAACACTGAAAACTCAG-3′; reverse 5′-CCGCTCGAGGTGATAAAAATAGAGTTCTTTTGTG-3′). Purified PCR products were T/A cloned into the pGEM-T vector (Promega). The caspase 3-FL cDNA was NdeI and XhoI digested from pGEM-T/cap3FL and ligated into the pET-23a vector (Novagen, Merck Bioscience). The aspartic acid residues of 9, 28, and 175 of pET-23a/caspase 3-FL were substituted to alanine using specific forward and reverse primers: D9A-f: 5′-CATATGGAGAACACTGAAAACTCAGTGCTTCAAAATCC; D28A-f: GAATCAATGGCCTCTGGAATA; D28A-r: GGATATTCCAGAGGCCATTGATTCGCT; D175A-f: GGCATTGAGACAGCCAGTGGTGTGAT; D175A-r: AACACCACTGGCTGTCTCAAT; and pET23a-121–143: TGTTAGCAGCCGGATCTCAGTGG. After PCR amplification, digestion and ligation, the pET-23a/caspase-3–3DA inactive mutant was produced.

Western Blotting, Immunoprecipitation, and GST Pulldown

Western blot analysis was performed as previously described (Tsai *et al.*, 2005; Wu *et al.*, 2005). For routine immunoprecipitation, cell extracts were adjusted to equal protein amount using lysis buffer. Cell extracts (1 mg protein in 350 μl lysis buffer) were incubated overnight with 2 μg specific antibody at 4°C with shaking. The resulting immunocomplexes were captured using protein A-Sepharose CL-4B beads (GE Healthcare) at 4°C for 1.5 h with shaking. The immunocomplexes were collected by centrifugation, washed three times with 1 ml of solution A (20 mM Tris-HCl, pH 7.0, and 0.5 mM dithiothreitol [DTT]) containing 0.5 M NaCl, and resuspended in 20 μl of solution A. For experiments used to identify PAK2-interacting proteins, cell extracts were further subjected to centrifugation at 100,000 × *g* for 30 min at 4°C before immunoprecipitation.

For the GST pulldown assay, His-tagged PAK2 and His-tagged MYO-18A-CB proteins were Ni-NTA–conjugated agarose column (QIAGEN, Chatsworth, CA) purified from BL-21 (DE3) cells (Promega Corporation) transformed with pET-15b-PAK2 and pET-15b-MYO18A-CB, respectively. GST-tagged MYO18A-CB, GST-tagged βPIX, and GST-tagged GIT1 were GSH-conjugated agarose column (GE Healthcare) purified from BL-21 (DE3) cells transformed with pGEX-3X/MYO18A-CB, pGEX-6P-bPIX, and pXJ40-GST-GIT1, respectively. To examine the interaction between MYO18A and PAK2, GST proteins or GST-tagged MYO18A-CB fusion proteins (500 ng) were mixed with lysis buffer containing 500 ng His-tagged PAK2 in a total volume of 0.5 ml. After incubation at 4°C for 3 h, the protein mixtures were immunoprecipitated with the indicated antibodies or control beads. The immunoprecipitated products were separated by SDS-PAGE, transferred to a PVDF membrane and probed with antibodies against the His-tag or GST-tag. To test the interaction between MYO18A and βPIX (or GIT1), 5 μg of GST-βPIX or GST-GIT1 were incubated with His-tagged MYO-18A-CB or inactive His-tagged caspase 3 (as control; 2 μg) in the binding buffer containing protease inhibitors (50 mM Tris-HCl, 150 mM NaCl, 0.1% Tween-20, 1 mM DTT, 1 mM leupeptin, 1 mM benzamidine, 1 mM phenylmethylsulfonyl fluoride, pH 7.5) at 4°C for 1 h, followed by incubation with GSH-Sepharose 4B at 4°C for another 1 h. The supernatants were removed by brief centrifugation, and the pellets were washed three times with buffer containing 20 mM Tris-HCl and 0.5 mM DTT). The resulting pellets were dissolved in 2× SDS-sample buffer, resolved in SDS-gels, and subjected to Western blotting. To pull down target proteins in cell lysates, 5 μg of GST-βPIX or GST-GIT1 immobilized on GSH-Sepharose 4B was incubated with A431 cell lysates (500 μg) in a total volume of 0.5 ml at 4°C for 2 h, and the proteins bound to GSH-beads were collected, washed, and subjected to Western blotting as described above.

RNA Interference

βPIX (ARHGEF7), GIT1, and control siRNA oligonucleotides were purchased from Dharmacon (Lafayette, CO) as follows: 5′-GAGCAUGAUUGAGCGGAUA-3′, 5′-UGAAUGUCCUCACGGAACA-3′, 5′-GGACGAGCUUUCCUUCUCA-3′, and 5′-GGAGGAUUAUCAUACAGAU-3′ (catalogue number L-009616; ON-TARGET plus SMART pool siRNA) for βPIX; 5′-GGACGACGCCAUCUAUUCA-3′, 5′-CGAGCUGCUUGUAGUGUAU-3′, 5′-CCGCACACCCAUUGACUAU-3′, and 5′-GCUCAGAGAAGAUCCAUUU-3′ (catalogue number L-020565; ON-TARGET plus SMART pool siRNA) for GIT1; and 5′-UGGUUUACAUGUCGACUAA-3′, 5′-UGGUUUACAUGUUGUGUGA-3′, 5′-UGGUUUACAUGUUUUCUGA-3′, and 5′-UGGUUUACAUGUUUUCCUA-3′ (catalogue number D-001810; ON-TARGET plus SMART pool siRNA) for nontargeting control siRNA. Transfection of siRNA oligonucleotides was performed using Lipofectamine RNAiMAX (Invitrogen) according to the provided protocol. For production of the MYO18A RNAi plasmids, three DNA oligos were constructed as follows: M1 5′-GATCCCCGAAAGACAAGGACAAAGATTTCAAGAGAATCTTTGTCCTTGTCTTTCTTTTTA-3′, M2 5′-GATCCCCGGCAGCTCAGCAGTTTAGTTCAAGAGAACTAAACTGCTGAGCTGCCTTTTTA-3′ and M3 5′-GATCCCCGTCGTGTCAGAAGAAGTTATTCAAGAGATAACTTCTTCTGACACACTTTTTA-3′ (the underlined sequences denote the sense or antisense sequences of MYO18A cDNA). These fragments were constructed in-house, using the pSuper.retro.puro vector backbone (OligoEngine, Seattle, WA) according to the provided protocol. Vector or RNAi plasmids were then transfected into A431 subclones (A431 S10) using Lipofectamine 2000 (Invitrogen) according to the manufacturer's protocol, to establish MYO18A-knockdown clones. Five hours after transfection, cells were subcultured and limited diluted into 96-well plates to obtain single clones, which were then selected using 1.6 μg/ml puromycin (InvivoGen, San Diego, CA). Clones established from the pSuper.retro.puro vector were designated V1 to V10, and clones established from pSuper.retro.puro/M1, pSuper.retro.puro/M2 and pSuper.retro.puro/M3 were designated M1-1 to M1-10, M2-1 to M2-10 and M3-1 to M3-10, respectively. Successful MYO18A-knockdown clones were identified by Western blot analysis of MYO18A protein expression.

Rescue Expression of EFGP-MYO18A in MYO18A-Knockdown Cells

To "rescue" the expression of MYO18A in MYO18A-knockdown cells, a rescue mutant of MYO18A (MYO18A-Rc) was generated by site-directed mutagenesis using a QuickChange site-directed mutagenesis kit (Stratagene, La Jolla, CA). pEGFP-C3/MYO18A was used as a template, and the primer used for site-directed mutagenesis had the sequence 5′-AGCTCAAGCTTCGAATTCCGATGTTTAACCTAATGAAAAAGGATAAAGATAAGGACGGCGGGCGGAAGGAGAAGA-3′, with the underlined bases representing the wobble positions to be mutated. The DNA sequence of the resulting Rc mutant was confirmed by autosequencing. The mutation of these nucleotides does not alter the amino acid sequence of MYO18A, but is expected to confer resistance to RNA interference in the M1 series of MYO18A-knockdown clones.

Immunostaining and Microscopy

A431 cells were cultured overnight on coverslips and then fixed with methanol for 5 min or with 4% formaldehyde for 15 min. Fixed cells were permeabilized in PBS containing 0.1% Triton X-100 and blocked by BSA (5 mg/ml in PBS). F-actin was visualized by staining with rhodamine– or fluorescein isothiocyanate (FITC)–phalloidin for 30 min. GIT1, MYO18A, and PAK2 were detected by incubation with specific antibodies and secondary antibodies conjugated with FITC or rhodamine, using the same protocol. The anti-PAK2 (V19) antibody was used for detection of PAK2 location. Cells were simultaneously stained with DAPI for visualization of nuclei. Focal adhesions were visualized by indirect immunofluorescence using an anti-vinculin antibody. Images were collected using a Leica TCS SP2 confocal laser scanning microscope (Leica Microsystems, Wetzler, Germany) with a 63× 1.32 NA oil immersion objective. The area and number of focal adhesions were determined using the NIH ImageJ software (ImageJ, http://rsb.info.nih.gov/ij/; Rasband, W. S., U. S. National Institutes of Health, Bethesda, MD/). For live cell imaging, cells transfected with paxillin-DsRed2 were plated on fibronectin (10 mg/ml)-coated 4.7-cm glass coverslips for 48 h. When the live image was recorded, coverslips were transferred to POC-R chamber (Zeiss, Jena, Germany) and maintained at 37°C and 5% CO_2, and the fluorescent cells were revealed by illumination with a halogen lamp. Images were acquired from a high-performance electron-multiplying CCD camera (EMCCD, Cascade: 512B, Photometrics, Roper Scientific, Tucson, AZ) attached to a Zeiss Axiovert 200M inverted microscope using 100× oil objective (Zeiss, Plan-Neofluar, 1.3 NA). Image acquisition was controlled with AxioVision 4.8 software (Zeiss). To detect DsRed2, filter sets of 15 from Zeiss were used. Exposure times ranged from 50 to 200 ms. To examine the fine structures of cell surface, cells were subjected to analysis by scanning electron microscopy (SEM). The scaffold was gold-coated and observed with SEM. S-5000 scanning electron microscope (Hitachi Science Systems, Tokyo, Japan) at an accelerating voltage of 15 kV.

Migration Assay

For wound-healing assays, confluent cell cultures grown in six-well plates were wounded by scraping with yellow pipette tips. Wound areas were marked and photographed at different time points using a digital camera attached to a phase-contrast microscope (Axioplan II, Zeiss). A transwell migration assay was performed using 24-well transwell plates containing 8-μm-pore-size polycarbonate filters (Corning Costar, Cambridge, MA). Cells (1×10^4) suspended in serum-free medium were added to the top chambers and incubated for 6 or 16 h, during which time-adhered cells were allowed to migrate toward 10 μg/ml collagen I (Sigma) as a chemoattractant in the lower chamber. Nonmigrant cells were removed with a cotton swab. Migrated cells on the underside of filters were methanol-fixed for 10 min, Giemsa-stained for 20 min, and counted under bright-field microscopy at a magnification of × 200, across 10 randomly selected fields.

Statistical Analysis

Where indicated, results were compared using the two-tailed *t* test. Differences were considered statistically significant when $p < 0.05$. All experiments were done independently at least three times, unless indicated otherwise.

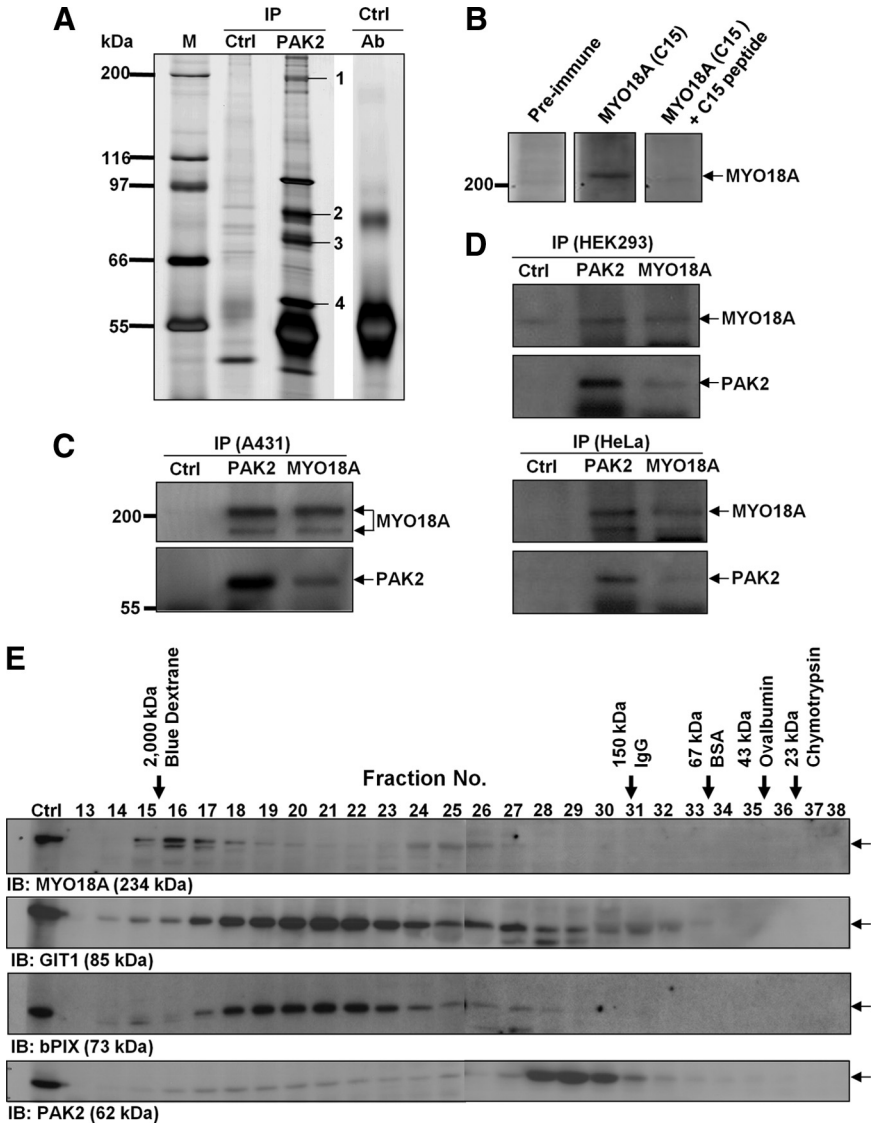

Figure 1. MYO18A is a PAK2-interacting partner. (A) A431 cell extracts (12 mg in 1 ml lysis buffer) were subjected to immunoprecipitation using 10 μg anti-PAK2 antibody and 150 μl of protein A-Sepharose CL-4B beads. To distinguish the specific interacting proteins from the background, 10 μg anti-PAK2 antibody alone (Ab ctrl) and the protein A bead–captured proteins from 12 mg A431 cell extracts (IP ctrl) were also analyzed in parallel. The immunoprecipitates and control samples were resolved by 8% SDS-PAGE, and the protein bands were detected by silver staining. Bands of interest were excised, in-gel–digested with trypsin, and analyzed by MALDI-TOF mass spectrometry, as described in *Materials and Methods*. Gel image shown is representative of three independent experiments. (B) A431 cell extracts (100 μg) were resolved by 8% SDS-PAGE and then immunoblotted (IB) separately with preimmune sera, anti-MYO18A (C15) antibody or anti-MYO18A (C15) antibody preincubated with the MYO18A C15 peptide, as detailed in *Materials and Methods*. (C) MYO18A (C15) or PAK2 (N17) antibodies were used to immunoprecipitate (IP) endogenous MYO18A protein from 1 mg of A431 cell lysate. The immunoprecipitates were resolved by 8% SDS-PAGE, transferred to PVDF membranes, and then probed with anti-MYO18A (C15) or PAK2 (N17) antibodies. Data shown are representative of three independent experiments. (D) HEK293 or HeLa cell lysates (1 mg each) were subjected to IP/IB experiments using anti-MYO18A (C15) or PAK2 (N17) antibodies, exactly as described in C. Similar results were obtained in three separate experiments. (E) A431 cell lysates (1 mg protein) were fractionated on a Superose 6 column, and the indicated fractions were subjected to immunoblotting with specific antibodies against MYO18A, GIT1, βPIX, and PAK2. Similar results were obtained in three separate experiments.

RESULTS

Identification of MYO18A as a PAK2-associated Protein

In an effort to identify and characterize novel PAK2-interacting proteins, we undertook an analysis of proteins coimmunoprecipitated with endogenous PAK2 (Figure 1A). The A431 human epidermoid carcinoma cell line was chosen as a model based on its abundant expression of PAK2 proteins. A431 lysates were immunoprecipitated with anti-PAK2 (N17) antibodies, the immunoprecipitates were resolved by SDS-PAGE, and silver staining was used to visualize the protein bands. Each band detected in the immunoprecipitates and prominently distinguishable from the background was excised and subjected to protein identification by MALDI-TOF mass spectrometry. The results of this mass spectrometric analysis are summarized in Table 1 and detailed in Supplemental Table S1. As expected, two previously reported PAK2-interacting proteins, GIT1 and βPIX, were identified (Figure 1A, bands 2 and 3, respectively, and Table 1). GIT1 proteins interact strongly with the PIX family of Rac1/Cdc42 GEFs, and thus indirectly with PAKs, which are PIX-binding partners (Manser *et al.*, 1998; Manabe *et al.*, 2002). These data authenticated the ability of our experimental procedures to identify PAK2-interacting proteins. In addition to these previously known binding partners, we identified an additional protein band of ~200 kDa, and subsequently identified the apparent PAK2-interacting protein as MYO18Aα (Figure 1A, band 1, and Table 1).

The myosin 18 proteins, the newest members of the myosin superfamily, comprise two subclasses: MYO18A and MYO18B (Berg *et al.*, 2001). The MYO18A gene encodes two different isoforms, MYO18Aα and MYO18Aβ (MYO18Aβ lacks the KE-rich region and PDZ domain found in

Table 1. Proteins identified in the PAK2-containing complexes immunoprecipitated from A431 cell lysates

Band no.	Protein	MW (kDa)	Mascot score	Sequence coverage rate (%)	Accession no.
1	MYO18A	234	245	25.4	Q92614
2	GIT1	85	184	42.6	Q9Y2X7
3	βPIX	73	64	23.2	Q14155
4	PAK2	62	86	28.6	Q13177

MYO18Aα), which have molecular weights of ~230 and 190 kDa, respectively (Mori *et al.*, 2003). The MYO18A variants localize to different cellular compartments, and their functions are not well understood (Furusawa *et al.*, 2000; Cross *et al.*, 2004; Isogawa *et al.*, 2005; Mori *et al.*, 2005). Northern blot analysis and RT-PCR data from Mori's group showed that MYO18Aα is present in most tissues, whereas MYO18Aβ is expressed specifically in hematopoietic tissues and cell lines (Mori *et al.*, 2003). To detect the endogenous protein level of MYO18A, we herein generated a rabbit anti-peptide antibody against the 15 amino acids at the carboxy terminus of MYO18A (the C15 peptide). As shown in Figure 1B, the C15 antibody recognized a specific protein band of ~200 kDa, and this signal could be selectively abolished by preincubating the antibody with C15 peptide before Western blotting. Notably, the C15 antibody was able to immunoprecipitate endogenous MYO18A from A431 cell lysates (Figure 1C). We then used the anti-C15 antibody to test the interaction of PAK2 and MYO18A in coimmunoprecipitation experiments and found that endogenous MYO18A could be coimmunoprecipitated with PAK2 and vice versa (Figure 1C). In addition to A431 cells, we also detected the interaction between PAK2 and MYO18A in other epithelial cell lines, including HEK293 and HeLa cells (Figure 1D), indicating that the interaction is real and specific.

Our C15 antibody could recognize both the α and β isoforms of MYO18A. In A431 cells, the amount of α-isoform (~230 kDa) was much higher than that of the β isoform (~190 kDa), which could only be clearly detected after immunoprecipitation (see Figure 1, B and C, for comparison). Our identification of the two MYO18A isoforms by the anti-C15 antibody is confirmed by the following: 1) a commercial antibody (N15) raised against an N-terminal peptide of the α isoform recognized the 230-kDa, but not the 190-kDa, protein band in immunocomplexes precipitated by the anti-C15 antibody (Supplemental Figure S1, A and B); and 2) the 230- and 190-kDa protein bands detected in the immunocomplexes pulled down by the anti-C15 antibody were identified by MALDI-TOF mass spectrometry (MS) as MYO18A isoforms α and β, respectively (Supplemental Figure S1, C–E, and Table S2). Collectively, these results demonstrate for the first time that MYO18A can interact with PAK2, and this might be a general fact in most epithelial cell types.

To further examine whether MYO18A and PAK2/βPIX/GIT1 form native complexes in cells, we separated A431 cell lysates on a gel filtration column and used Western blotting to detect the four proteins in each of the resulting fractions (Figure 1E). Our gel filtration data suggest that all four proteins are dimeric or multimeric under general conditions, which are consistent with that from previous studies. (Premont *et al.*, 2004; Isogawa *et al.*, 2005; Hoefen and Berk, 2006). The gel filtration experiments revealed that we could detect coelution of GIT1, βPIX, and PAK2 across a wide range of molecular weight sizes (fractions 16–30), although GIT1 and βPIX were enriched in the higher molecular weight fractions (16–26) and PAK2 was enriched in the lower molecular weight fractions (28–31). Notably, MYO18A cofractionated with GIT1 and βPIX in fractions with very high (fractions 16–20) and lower (fraction 24–27) molecular weight sizes, but had little overlap with the PAK2 signal (Figure 1E). The gel filtration data are consistent with the notion that MYO18A might interact directly with GIT1 and/or βPIX, but not PAK2, to form PAK2/βPIX/GIT1/MYO18A complexes. As the bulk of MYO18A exists in a very high molecular weight complex (larger than GIT1/βPIX complex), and there is only a small fraction of PAK2 at this molecular-weight range, the binding of PAK2 to both the GIT1/βPIX complex and the higher molecular weight GIT1/βPIX/MYO18A complex seems to be unstable.

MYO18A Participates in PAK2-containing Complexes via Its C-Terminus

To dissect the structural basis of the interaction between MYO18A and the PAK2-containing complexes, we next sought to map the domain(s) of MYO18A participating in this interaction. As mentioned, MYO18Aα (the major isoform expressed in A431 cells) contains a KE-rich region, an N-terminal PDZ domain, and a characteristic myosin homology region of head, neck (with one IQ motif), and coiled-coil tail (Supplemental Figure S1A). Full-length MYO18Aα and several of its deletion mutants (Figure 2A) were designed according to the predicted domains, cloned into pCMV-Myc or pEGFP-C3 vectors, and expressed separately in A431 cells (Figure 2B). The resulting cell lysates were subjected to immunoprecipitation using anti-PAK2 (N17) or anti-Myc antibodies. We found that the Myc-tagged MYO18A-FL and MYO18A-C, but not MYO18A-N, could be coimmunoprecipitated with PAK2, suggesting that the carboxy terminus (including the coiled-coil tail) of MYO18Aα is crucial for this interaction (Figure 2C). To explore this interaction further, four smaller mutants were derived from the MYO18A-C mutant (MYO18A-CA, -CB, -CB-L, and -CB-S) and used for coimmunoprecipitation experiments. Only the MYO18A-CB and MYO18A-CB-S mutants coimmunoprecipitated with PAK2 (Figure 2, D–F), indicating that the most C-terminal part (amino acids 1972–2054) of MYO18Aα is important for this interaction.

MYO18A Does Not Interact Directly with PAK2 In Vitro

Because the C-terminus of MYO18A is critical for its binding to the PAK2-containing complexes, we tested whether MYO18A can bind to PAK2 directly in vitro. Recombinant His-tagged PAK2 and GST fusion proteins containing the CB domain of MYO18A (GST-MYO18A-CB) were produced in *Escherichia coli.* The purified recombinant His-tagged PAK2 (His-PAK2) retained its ability to interact with MYO18A, as evidenced by the observation that His-PAK2 could be coimmunoprecipitated with endogenous MYO18A from A431 cell lysates and vice versa (Supplemental Figure S2, A and B). We then tested the interaction between His-PAK2 and GST-MYO18A-CB in vitro. Purified GST-MYO18A-CB or GST alone (negative control) was immobilized to glutathione-Sepharose 4B beads. This affinity matrix was incubated with purified His-PAK2, and the anti-His antibody was used to detect the interaction. However, we could not detect binding of His-PAK2 to GST-MYO18A-CB (Supplemental Figure S2C). These data suggest that the interaction of MYO18A to PAK2 is not a direct binding and may occur through one or more adaptor protein(s).

βPIX Interacts Directly with MYO18A In Vitro and Plays Critical Role in PAK2/βPIX/GIT1/MYO18A Complex Formation In Vivo

Because the GIT1 and βPIX proteins are known PAK-interacting proteins and were also detected in the PAK2 immunocomplexes (Figure 1A), we speculated that these proteins might act as scaffolds for the physical link between MYO18A and PAK2. To examine this possibility, we used GST-pull down assay to investigate the interaction between MYO18A and βPIX/GIT1 complexes. Recombinant His-tagged MYO18A-CB (Figure 3A) and GST fusion proteins containing βPIX and GIT1 (GST-βPIX and GST-GIT1;

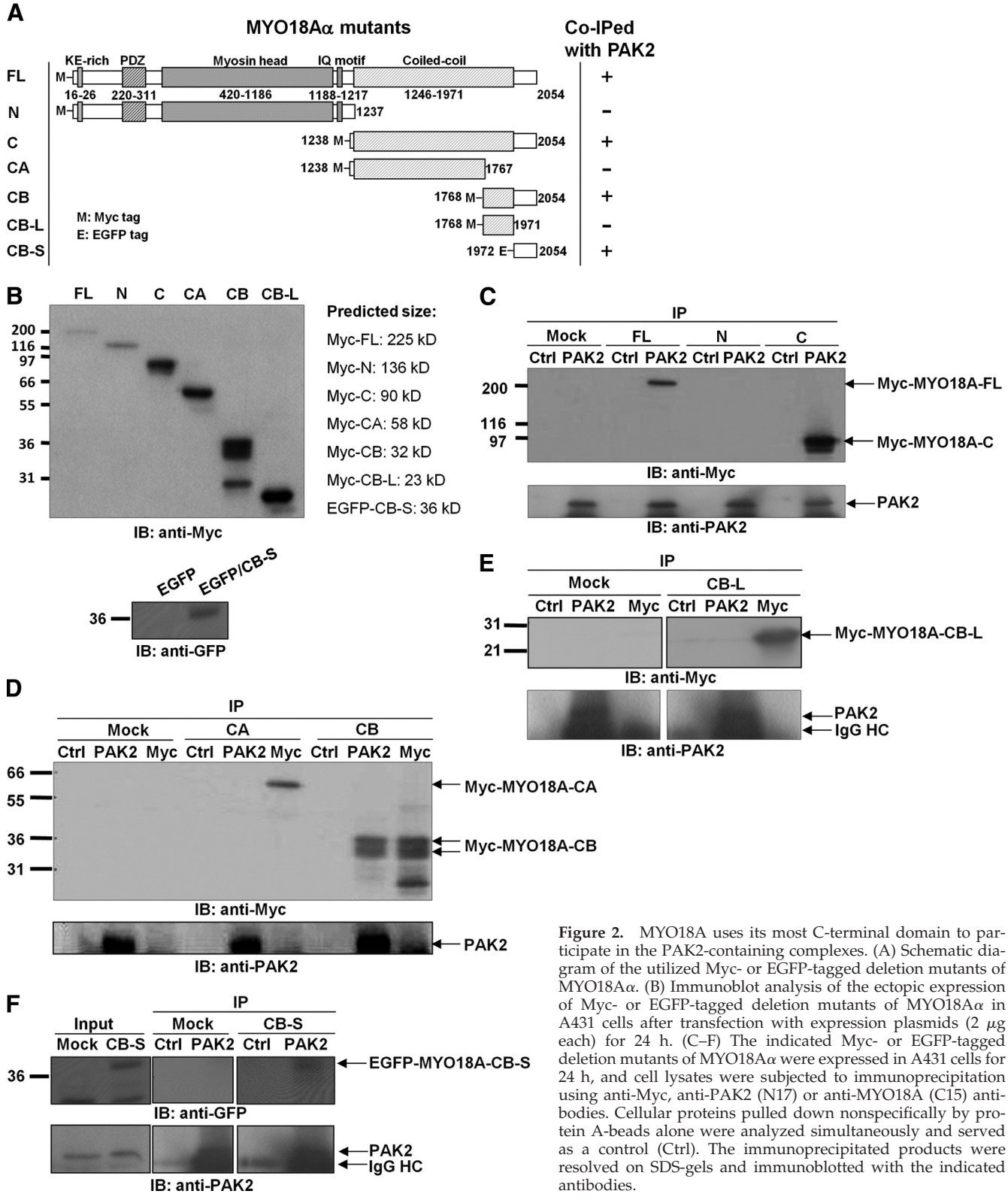

Figure 2. MYO18A uses its most C-terminal domain to participate in the PAK2-containing complexes. (A) Schematic diagram of the utilized Myc- or EGFP-tagged deletion mutants of MYO18Aα. (B) Immunoblot analysis of the ectopic expression of Myc- or EGFP-tagged deletion mutants of MYO18Aα in A431 cells after transfection with expression plasmids (2 μg each) for 24 h. (C–F) The indicated Myc- or EGFP-tagged deletion mutants of MYO18Aα were expressed in A431 cells for 24 h, and cell lysates were subjected to immunoprecipitation using anti-Myc, anti-PAK2 (N17) or anti-MYO18A (C15) antibodies. Cellular proteins pulled down nonspecifically by protein A-beads alone were analyzed simultaneously and served as a control (Ctrl). The immunoprecipitated products were resolved on SDS-gels and immunoblotted with the indicated antibodies.

Figure 3C) were produced in E Coli and then affinity-purified. The His-tagged caspase 3 was also produced and purified as a negative control for the pulldown assay (Figure 3A). The purified recombinant GST-βPIX and GST-GIT1 retained the ability to bind to each other from A431 cell lysates (Figure 3, D and E, middle). We then examined the direct interaction between His-MYO18A-CB and GST-βPIX (or GST-GIT1) in vitro. Purified His-MYO18A-CB or His-caspase 3 (negative control) was first incubated with purified GST protein alone to exclude the nonspecific binding

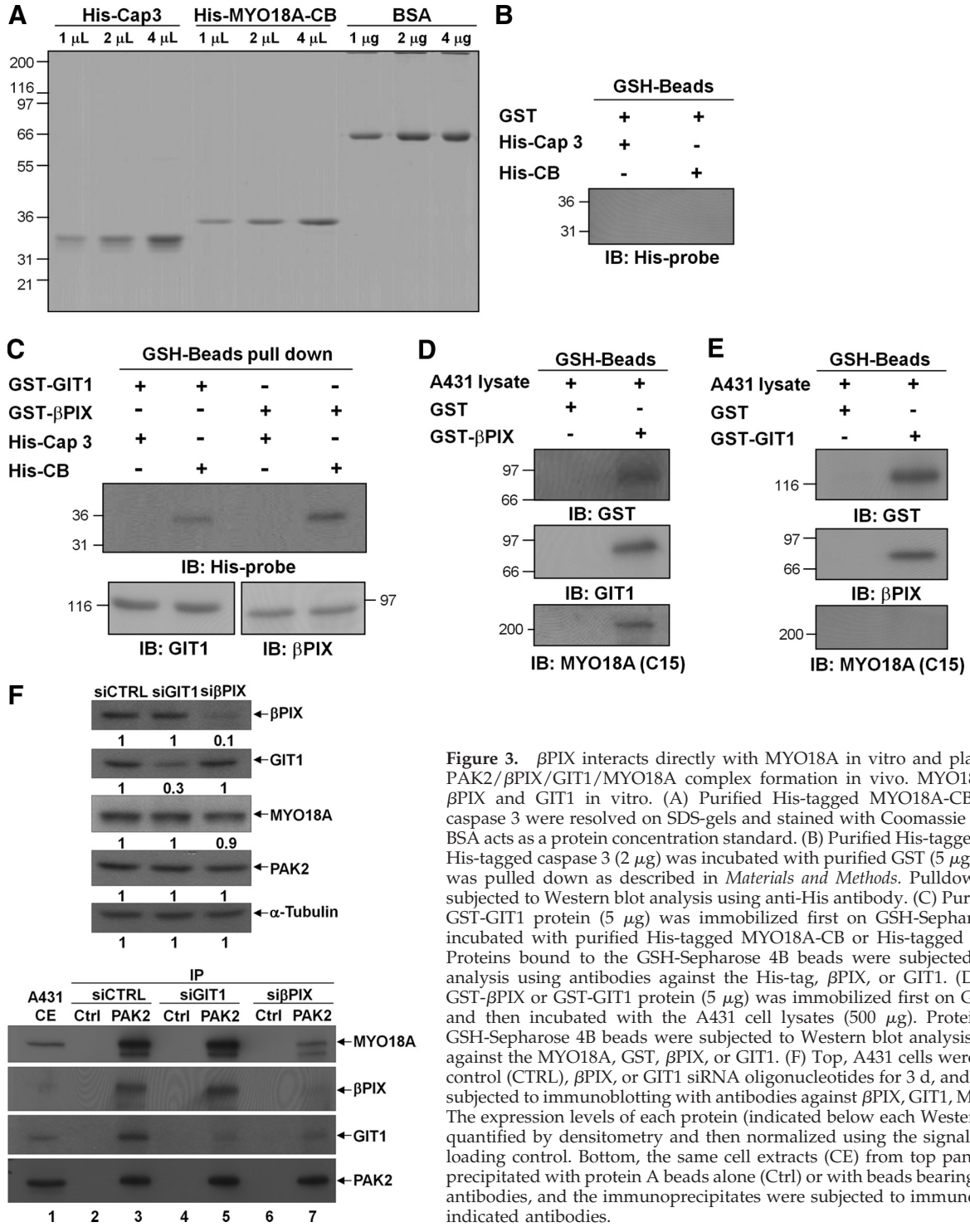

Figure 3. βPIX interacts directly with MYO18A in vitro and plays critical role in PAK2/βPIX/GIT1/MYO18A complex formation in vivo. MYO18A interacts with βPIX and GIT1 in vitro. (A) Purified His-tagged MYO18A-CB and His-tagged caspase 3 were resolved on SDS-gels and stained with Coomassie blue as indicated. BSA acts as a protein concentration standard. (B) Purified His-tagged MYO18A-CB or His-tagged caspase 3 (2 μg) was incubated with purified GST (5 μg), and the mixture was pulled down as described in *Materials and Methods*. Pulldown products were subjected to Western blot analysis using anti-His antibody. (C) Purified GST-βPIX or GST-GIT1 protein (5 μg) was immobilized first on GSH-Sepharose 4B and then incubated with purified His-tagged MYO18A-CB or His-tagged caspase 3 (2 μg). Proteins bound to the GSH-Sepharose 4B beads were subjected to Western blot analysis using antibodies against the His-tag, βPIX, or GIT1. (D and E) Purified GST-βPIX or GST-GIT1 protein (5 μg) was immobilized first on GSH-Sepharose 4B and then incubated with the A431 cell lysates (500 μg). Proteins bound to the GSH-Sepharose 4B beads were subjected to Western blot analysis using antibodies against the MYO18A, GST, βPIX, or GIT1. (F) Top, A431 cells were transfected with control (CTRL), βPIX, or GIT1 siRNA oligonucleotides for 3 d, and cell extracts were subjected to immunoblotting with antibodies against βPIX, GIT1, MYO18A, or PAK2. The expression levels of each protein (indicated below each Western blot data) were quantified by densitometry and then normalized using the signal of α-tubulin as a loading control. Bottom, the same cell extracts (CE) from top panel were immunoprecipitated with protein A beads alone (Ctrl) or with beads bearing anti-PAK2 (N17) antibodies, and the immunoprecipitates were subjected to immunoblotting with the indicated antibodies.

effect (Figure 3B). Then His-MYO18A-CB or His-caspase 3 was incubated with GST-βPIX or GST-GIT1, and the complexes pulled down by GSH-beads were subjected to Western blot analysis using anti-His antibody. The result showed that His-MYO18A-CB could interact with both GST-βPIX and GST-GIT1 in vitro, with a higher amount (about two-fold) of His-MYO18A-CB detected in the complexes pulled down by GST-βPIX (Figure 3C). As equal amounts of GST-βPIX and GST-GIT1 fusion proteins were used as the baits to pull down a fixed amount of His-MYO18A-CB, the result implicates that the in vitro interaction between βPIX and MYO18A could be stronger than that between GIT1 and MYO18A. Moreover, when using equal amounts of GST-βPIX and GST-GIT1 fusion proteins as the baits, only GST-βPIX, but not GST-GIT1, could pull down authentic MYO18A from A431 cell lysates (Figure 3, D and E, bottom). Collectively, these observations indicate that MYO18A can directly bind to βPIX via its C-terminal part in vitro.

To further investigate the role of βPIX in mediating the formation of PAK2/βPIX/GIT1/MYO18A complexes in vivo, we applied siRNA technology to knock down the βPIX expression in A431 cells and then examined the effect of βPIX depletion on the PAK2/βPIX/GIT1/MYO18A complexes. Meanwhile, knockdown of GIT1 was also performed in parallel for comparison. As shown in Figure 3F, the protein levels of both GIT1 and βPIX were effectively reduced in A431 cells by their respective siRNA after a 3-d transfection. In general, transient knockdown of GIT1 or βPIX had little effect on the expression of βPIX, MYO18A, or PAK2, although knockdown of βPIX caused a small reduction of the MYO18A protein levels (Figure 3F). Lysates of GIT1- or βPIX-knockdown cells were then subjected to immunoprecipitation by anti-PAK2 antibodies, and the immunocomplexes were analyzed by immunoblotting with antibodies against GIT1, βPIX, MYO18A, or PAK2. As we expected, GIT1 and βPIX signals were clearly detected in immunoprecipitates pulled down from control cell lysates by antibodies against PAK2 (Figure 3F, lane 3). In GIT1-knockdown cells, the level of MYO18A and βPIX remained almost unchanged in immunoprecipitates pulled down by the anti-PAK2 antibody (Figure 3F, lane 5). In contrast, when βPIX was knocked down, the amounts of MYO18A and GIT1 were greatly reduced in immunocomplexes precipitated by the PAK2 antibody (Figure 3F, lane 7). Collectively, these observations indicate that the interaction between MYO18A and PAK2 is mediated through the βPIX/GIT1 complex, and also indicate that βPIX plays a critical role in maintaining the PAK2/βPIX/GIT1/MYO18A complexes in cells.

PAK2 Binds to MYO18A via Its Regulatory Domain through the βPIX/GIT1 Complex

To further map the region of PAK2 that participates in formation of the PAK2/βPIX/GIT1/MYO18A complexes, we expressed the Myc-tagged full-length, N-terminal regulatory domain or C-terminal catalytic domain of PAK2 in A431 cells and performed coimmunoprecipitation experiments using the antibody against MYO18A. Our results showed that ectopically expressed full-length PAK2 and its N-terminal regulatory domain, but not its C-terminal catalytic domain, coimmunoprecipitated with endogenous MYO18A (Figure 4, A–C). Because the N-terminal regulatory domain of PAK2 has been reported as the region for βPIX/GIT1 binding (Obermeier *et al.*, 1998, Koh *et al.*, 2001), we then generated a mutant of PAK2, PAK2-P185G/R186A, which has been reported to lose binding activity to βPIX (Renkema *et al.*, 2001), and used this mutant to confirm whether the interaction of PAK2 with MYO18A was through the βPIX/GIT1 complex. We expressed the Myc-tagged full-length and mutant form of PAK2 in A431 cells, and used the anti-Myc antibody to perform coimmunoprecipitation experiments (Figure 4D). As expected, Western blotting data confirmed that βPIX could no longer be coimmunoprecipitated with the PAK2-P185G/R186A mutant from cell lysates; under this circumstance, the amounts of MYO18A also decreased drastically in the immunocomplexes (Figure 4D, cf. lanes 4 and 6). Taken together, these observations indicate that PAK2 interacts with MYO18A through the βPIX/GIT1 complexes.

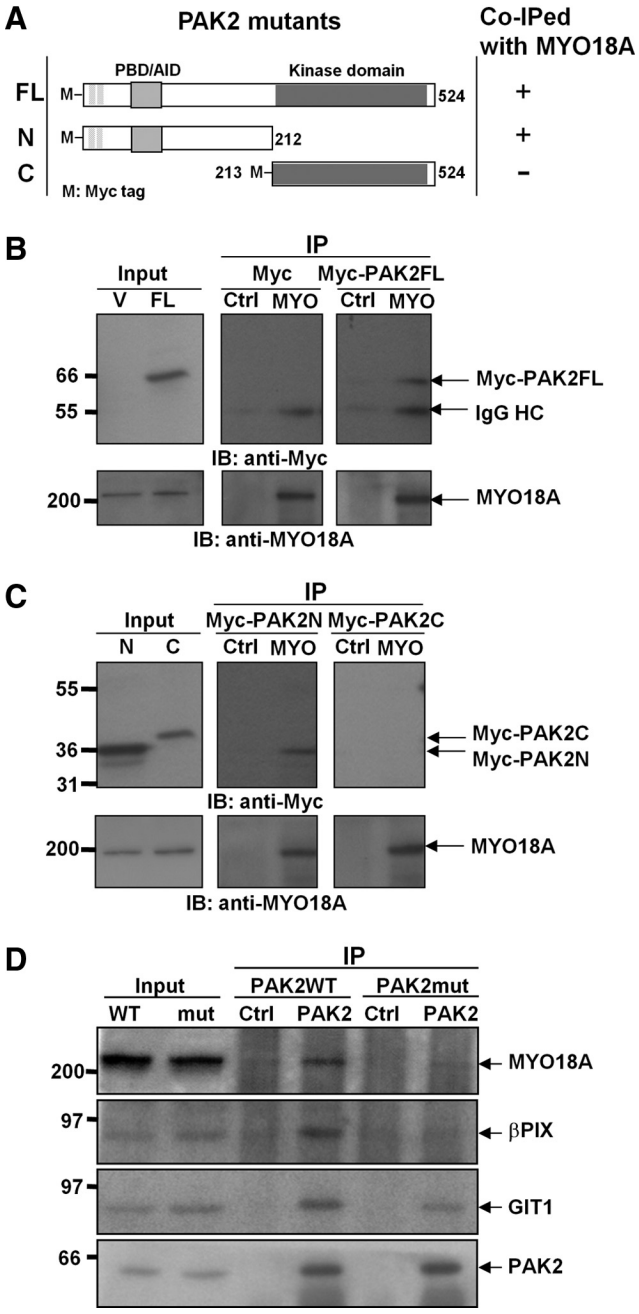

Figure 4. PAK2 binds to MYO18A through its N-terminal regulatory domain. (A) Schematic diagram of the utilized Myc-tagged deletion mutants of PAK2. (B–D) Myc-tagged, full-length deletion mutants and P185G, R186A mutant of PAK2 were expressed in A431 cells for 24 h, and cell lysates were subjected to immunoprecipitation using anti-MYO18A (C15) antibodies. Cellular proteins pulled down nonspecifically by protein A-beads alone were analyzed simultaneously and served as a control (Ctrl). Immunoprecipitated products were resolved on SDS-gels and immunoblotted with the indicated antibodies.

Formation of PAK2/βPIX/GIT1 Complexes Occurs in a MYO18A-independent Manner

We have shown that MYO18A is a new PAK2/βPIX/GIT1 interacting partner. As PAK/βPIX/GIT1 complex-mediated signaling has been well established and is believed to participate in numerous biological processes, we next sought to investigate the role of MYO18A in the regulation of the PAK/βPIX/GIT1 complex. We first examined the effect of siRNA-mediated knockdown of MYO18A on PAK/βPIX/GIT1 complex formation in A31 cells. Three vector-based siRNA constructs (siM1–siM3) were tested; siM1 appeared most effective in reducing MYO18A protein levels after tran-

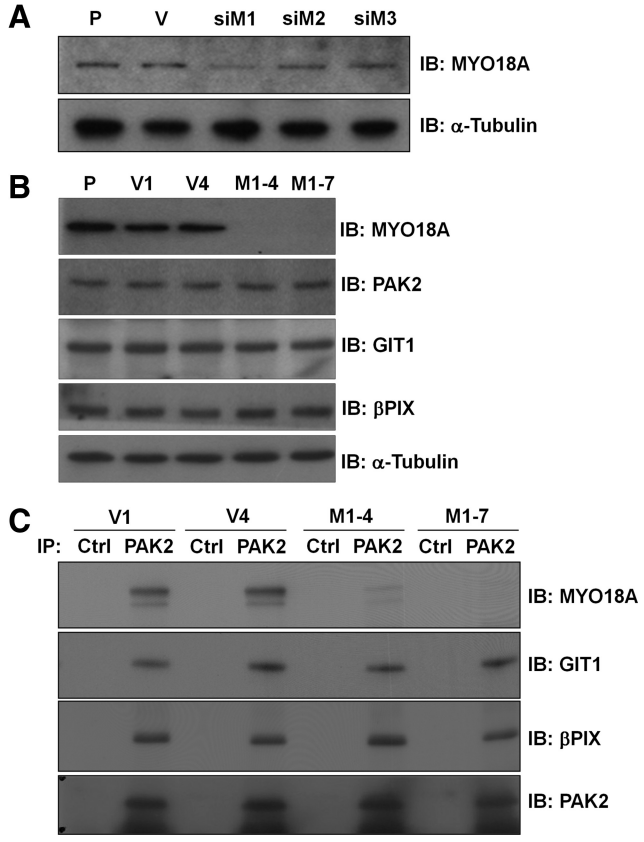

Figure 5. Formation of PAK2/GIT1/βPIX complexes does not require the presence of MYO18A. (A) A431 cells were transfected with vector control (V) or pSuper/MYO18A siRNA constructs (siM1, siM2, and siM3), as detailed in *Materials and Methods.* At 48 h after transfection, the expression levels of MYO18A were determined by immunoblotting. P, nontransfected parental A431 cells. (B) Expression levels of MYO18A, PAK2, GIT1, and βPIX in two siRNA vector control clones (V1 and V4) and two MYO18A stable knockdown clones (M1-4 and M1-7) were analyzed by immunoblotting with the appropriate antibodies. The α-tubulin signal was used as a loading control. (C) Lysates of the four cell clones were immunoprecipitated with anti-PAK2 (N17) antibodies, and the immunoprecipitates were immunoblotted with the indicated antibodies. The data shown are representative of three independent experiments.

sient transfection (Figure 5A) and was further used to successfully establish MYO18A stable knockdown clones M1-4 and M1-7 (Figure 5B, compare with the two siRNA vector control clones, V1 and V4). Knockdown of MYO18A had little effect on the protein levels of PAK2, GIT1, or βPIX (Figure 5B). Immunoprecipitation of endogenous PAK2 from the four cell clones revealed that the depletion of MYO18A had a little effect on the formation of PAK2/βPIX/GIT1 complexes in A431 cells (Figure 5C), suggesting that formation of PAK2/GIT1/βPIX complexes occurs in a MYO18A-independent manner.

MYO18A and PAK2 Colocalize in Membrane Ruffles

Having shown that MYO18A is a novel PAK2-binding partner, we next investigated how this protein might influence the cellular functions of PAK2. According to previous studies, PAK2 can be located at various subcellular sites, including the ER, membranes, cytosol, and nucleus (Brown *et al.*, 2002; Huang *et al.*, 2003). In contrast, MYO18A codistributes with actin fibers and localizes to the inner surface of the cell membrane (Mori *et al.*, 2005). Here, we first visualized the localization of both PAK2 and F-actin in A431 cells, using double immunofluorescence and confocal microscopy. As shown in Figure 6A, PAK2 localized not only within the cytoplasm, but also at the membrane ruffles and lamellipodia where F-actin massively accumulated. Then, we costained PAK2 and MYO18A in cells, which showed that MYO18A distributed within the cytoplasm and in membrane ruffles (Figure 6B, top), as previous described (Mori *et al.*, 2003). Image overlay indicated that the two proteins partially colocalized within the cytoplasm but significantly colocalized at membrane ruffles. The specificities of the two antibodies (the anti-MYO18A [N15] antibody and anti-PAK2 [V19] antibody) were confirmed by immunoprecipitation and/or immunoblotting experiments (Supplemental Figures S1B and S3A, respectively). Analysis of enlarged images further revealed that PAK2 was enriched in both membrane ruffles and lamellipodia, whereas MYO18A was apparently concentrated in the ruffles (Figure 6B, middle and bottom). The colocalization of PAK2 and MYO18A at membrane ruffles was further examined in A431 cells ectopically expressing EGFP-MYO18A. Immunoblot analysis showed that EGFP-MYO18A was expressed at the predicted molecular size and at a level similar to that of endogenous MYO18A (Supplemental Figure S3B). Consistent with the localization of endogenous MYO18A, the ectopically expressed EGFP-MYO18A was located at both membrane ruffles and in the cytoplasm, and showed a significant colocalization with PAK2 at membrane ruffles (Figure 6C). Again, a notable distribution of PAK2 at lamellipodia was observed in these EGFP-MYO18A-expressing cells (Figure 6D and Supplemental Figure S3, C–E).

Depletion of MYO18A Increases Actin Stress Fiber Density and Focal Adhesion Formation and Alters GIT1 and PAK2 Localization

Although MYO18A depletion had no significant effect on the protein levels and formation of PAK2/βPIX/GIT1 complexes, the MYO18A-knockdown cells were more spread and had a notably enlarged and flattened morphology (Figure 7A). Meanwhile, SEM data revealed that the MYO18A-knockdown cells have obviously less ruffles and dorsal filopodia compared with the control cells (Figure 7C). This observation suggested that the actin filaments and/or focal contacts of A431 cells may be altered when MYO18A is knocked down. Staining of control and MYO18A-depleted cells with FITC-phalloidin (for visualization of actin stress fibers) and antibodies against vinculin (to detect focal adhesions) revealed that both actin stress fibers were drastically increased and focal adhesion area were larger in MYO18A-knockdown cells (Figure 7D and Supplemental Figure S4). Like GIT1, the protein level of vinculin did not change when MYO18A was knocked down (Figure 7B). Quantification revealed that knockdown of MYO18A resulted in an approximately twofold increase in the number of focal adhesions and an approximately fourfold enlargement of their size, compared with focal adhesions in control cells (Figures 7, E and F). However, although cells with depletion of MYO18A has a slightly higher percentage of cell area containing focal adhesion in average than that of control cells, the difference was not statically significant (Figure 7G). We also found that loss of MYO18A in cells enhanced the accumulation of GIT1 to focal contacts, similar to that of vinculin (Figure 7H and Supplemental Figure S5). Costaining of GIT1 and vinculin in both control and MYO18A knockdown cells further revealed that the patterns of GIT1 and vinculin distribution merged very well in both control and MYO18A-knockdown cells,

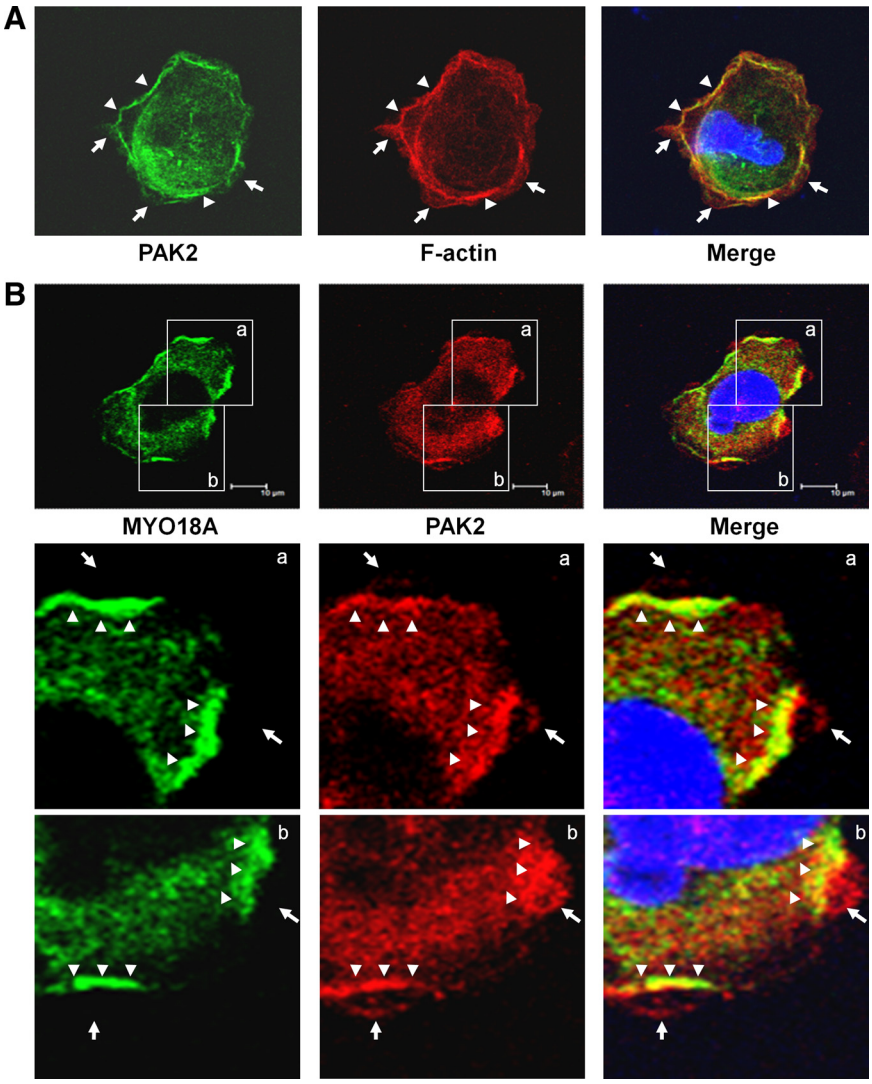

Figure 6. MYO18A and PAK2 colocalize in membrane ruffles. (A) A431 cells were grown on coverslips, fixed, costained with Texas Red-phalloidin (for visualization of F-actin) and anti-PAK2 (V19) antibodies, and observed under a Leica confocal microscope. Arrows and arrowheads indicate the positions of selected lamellipodia and membrane ruffles, respectively. (B) As in A except the cells were immunostained for both MYO18A and PAK2 using anti-MYO18A (N15) and anti-PAK2 (V19) antibodies. The boxed images in the top panel are enlarged and shown in the middle and bottom panels. The symbols used are as in A. (C) A431 cells were transfected with pEGFP-C3/MYO18A for 24 h and immunostained using an anti-PAK2 (V19) antibody followed by a rhodamine-conjugated secondary antibody. Images for EGFP-MYO18A (green) and endogenous PAK2 (red) were obtained using a Leica confocal microscope. (D) Enlarged images of the boxed areas from C. The symbols used are as in A.

and the ratio of vinculin to GIT1 did not change significantly in the two cell types (Supplemental Figure S6). This observation suggests that MYO18A depletion affects the structure of focal adhesions rather than the ratio of vinculin to GIT1. Because depletion of MYO18A did not affect the formation of PAK2/βPIX/GIT1 complexes (Figure 5C), we investigated whether the localization of PAK2 was altered in MYO18A-knockdown cells. Remarkably, immunostaining showed that although the cellular levels of PAK2 remained unchanged in MYO18A-depleted cells, much less PAK2 was distributed to membrane ruffles in knockdown versus control cells, whereas more of the protein accumulated at the focal adhesions; this is in line with the GIT1 staining results obtained in MYO18A-depleted cells (Figure 7I and Supplemental Figure S7). Collectively, these results suggest that MYO18A plays a critical role in regulating actin stress fiber and membrane ruffle formation, as well as PAK2/βPIX/GIT1 complex localization in cells.

MYO18A Is Required for A431 Cell Migration

Focal adhesions need to turn over to allow the cell to move forward, and cells with high migration ability tend to have many smaller focal adhesions that turn over rapidly (Lock *et al.*, 2008). To evaluate the turnover rate of focal adhesions in both control and MYO18A-knockdown cells, we transfected a DsRed2-paxillin plasmid into both cells and recorded the live image data when DsRed2-paxillin was expressed and incorporated in to focal adhesions. The results from time-lapse video showed that the focal adhesion turnover rate was much lower in MYO18A-depleted cells compared with that of control cells (Movies S1–S4). To investigate the effect of MYO18A depletion-induced alterations of actin stress fibers and focal adhesions, we then examined the migration ability of MYO18A-depleted and control cells. The results from our wound-healing assay showed that MYO18A-knockdown M1-7 cells migrated much more slowly than vector control V4 cells (Figure 8A). A transwell migration assay further revealed that far fewer M1-4 and M1-7 cells migrated to the lower chamber, compared with V1 and V4 cells (Figure 8B). To examine whether reexpression of MYO18A into MYO18A-knockdown cells could rescue their migration ability, we constructed a rescue mutant (Rc-mut) by site-directed mutagenesis of wild-type pEGFP-C3/MYO18A, as described in *Materials and Methods*. As shown in Figure 8C, this Rc-mut expressed EGFP-MYO18A at the predicted size in M1-7 cells, whereas no detectable signal could be observed after transfection of the wild type plasmid, confirming both that the RNAi was highly effective in M1-7 cells,

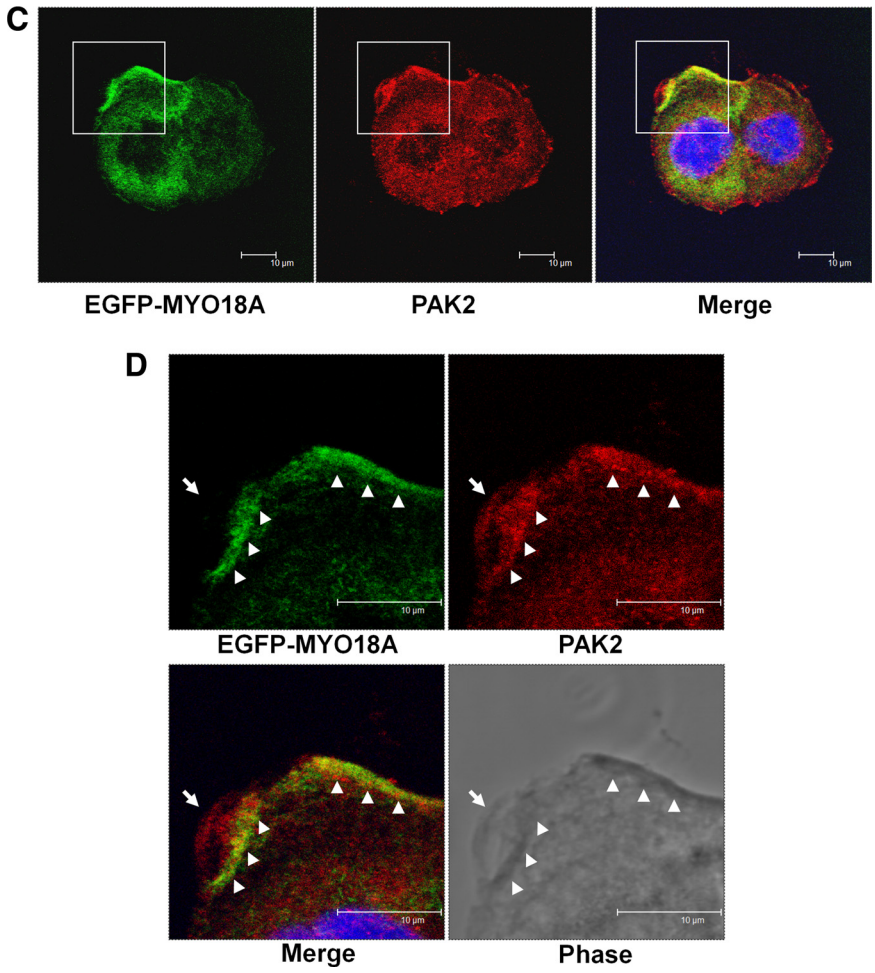

Figure 6. *Continued.*

and that it was feasible to reexpress MYO18A using the rescue mutant in these cells. However, as the MYO18A-depleted cells are fragile and sensitive to transfection, the levels of reexpressed MYO18A in these cells are usually not comparable to that of vector control cells. When MYO18A was reexpressed in M1-7 cells, their transwell migration ability was significantly enhanced (reaching ~71% of the level seen in V1 vector control cells), although its expression can only reach ~40% of the level detected in control cells (Figure 8, D and E). These results indicate that MYO18A is required for A431 cell migration, and suggest that MYO18A may regulate cell motility through controlling actin filaments, membrane ruffles and focal adhesions.

DISCUSSION

To date, more than 40 different kinase substrates of activated PAKs have been reported (Bokoch, 2003; Kumar *et al.*, 2006). These substrates consist of a diverse group of proteins, many of which are known to participate in regulation of the cytoskeleton. However, increasing evidence indicates that some aspects of the PAK-mediated regulation of cytoskeletal reorganization and cell motility do not require PAK kinase activity (Sells *et al.*, 1999; Bokoch, 2003; Zegers, 2008). In this work, using a proteomic approach, we demonstrate for the first time that MYO18A is a novel binding partner of the PAK2/βPIX/GIT1 complex and suggest that MYO18A may play an important role in mediating PAK2/βPIX/GIT1 complex localization and epithelial cell migration. The results presented herein provide several important links between PAK2 and the unconventional myosin, MYO18A.

First, we demonstrated that MYO18A interacts with PAK2 via the formation of PAK2/βPIX/GIT1/MYO18A complexes and found that this may be a general fact in most epithelial cells (Figure 1). Our data also suggest that MYO18A participates in PAK2-interacting protein complexes through the GIT1/βPIX complex, but depletion of MYO18A did not affect the ability of PAK2 to bind to the complex. As numerous studies have reported that many functions of PAK depend on its ability to bind to PIX (Zegers, 2008), our present findings provide a new case that βPIX is required for the interaction between PAK2 and MYO18A (Figures 3 and 4). Because isoforms of PAK and GIT exist in human cells, it is possible that these isoforms, such as PAK1 and GIT2, may also form complex with MYO18A. To test this possibility, we have examined the interaction between PAK1 and MYO18A by the same assay condition used for coimmunoprecipitation of PAK2 and MYO18A. To our surprise, however, we found that PAK1 and MYO18A could not be coimmunoprecipitated with each other (data not shown), suggesting that the PAK/PIX/GIT/MYO18A complexes might be formed in an isoform-specific manner. The reason for this phenomenon is currently unknown. On the basis of this observation, whether different isoforms of PAK, GIT, or PIX are present in this complex or not should be tested one by one.

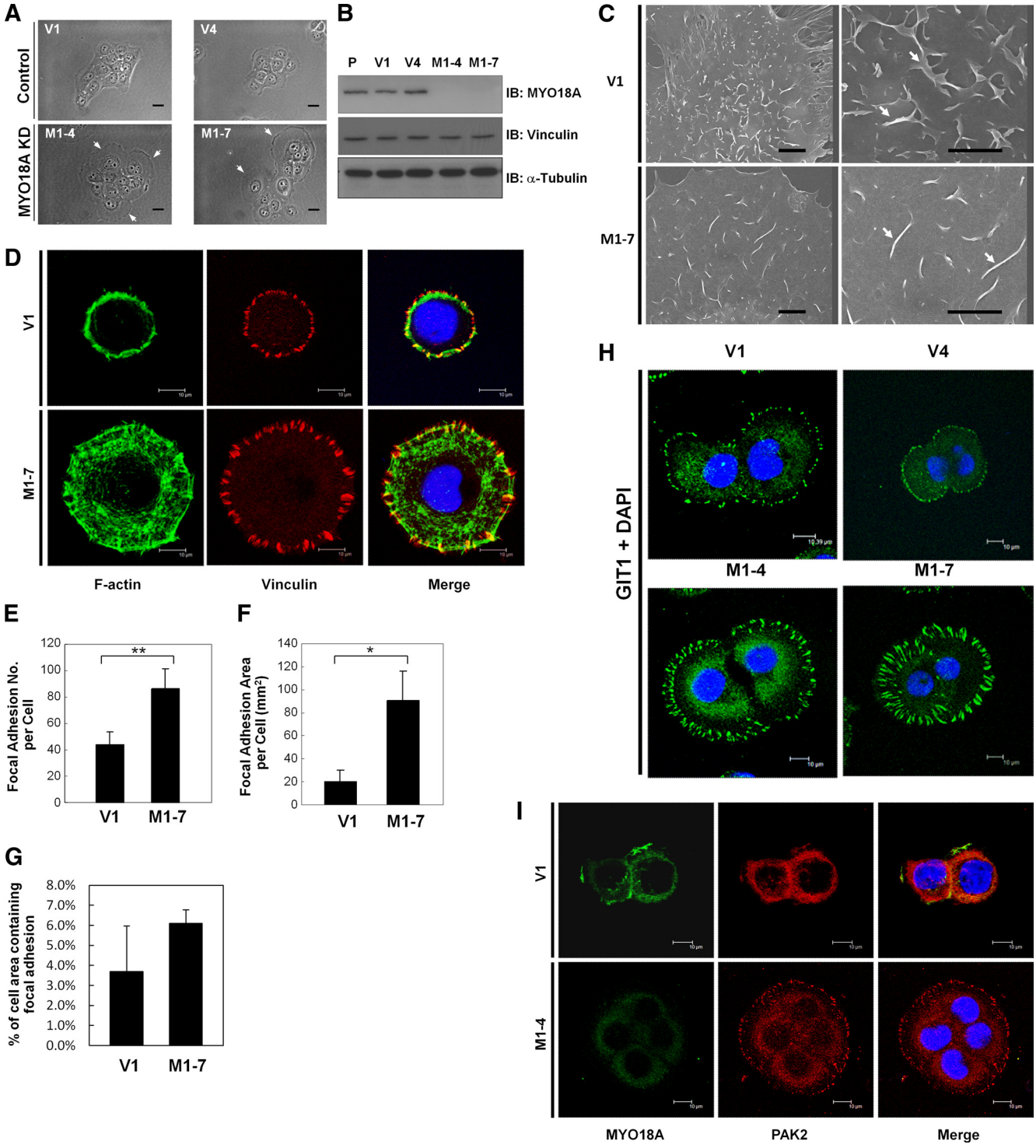

Figure 7. Depletion of MYO18A alters the localization of GIT1 and PAK2 and changes focal adhesions. (A) The representative morphologies of control and MYO18A-knockdown cells. Scale bar, 20 μm. (B) Expression levels of vinculin, a focal adhesion marker, in parental (P), control (V1 and V4), and MYO18A-knockdown cells (M1-4 and M1-7). (C) SEM photogram of control (V1) and MYO18A-knockdown cells (M1-7). Scale bar, 3 μm, and arrows indicate the ruffles. (D) Control and MYO18A-knockdown cells were fixed and stained using FITC-phalloidin (for visualization of F-actin) and anti-vinculin antibodies (to detect focal adhesions) (D). The number (E) and size (F) of focal adhesions per cell and the percentage of cell area containing focal adhesion (G) were quantified as described in *Materials and Methods*. Data shown represent the mean ± SEM of data for at least six cells. *$p < 0.005$; **$p < 0.0005$ (two-tailed *t* test). (H and I) Experiments performed as in D, with anti-GIT1 (H), anti-MYO18A or anti-PAK2 antibodies (I) used for cell staining. Images shown are representative of three separate experiments.

Second, our data clearly showed the colocalization of PAK2 and MYO18A in cells, especially at lamellipodia and membrane ruffles (Figure 6). According to previous studies, PAK2 may be found in various intracellular locations, in-

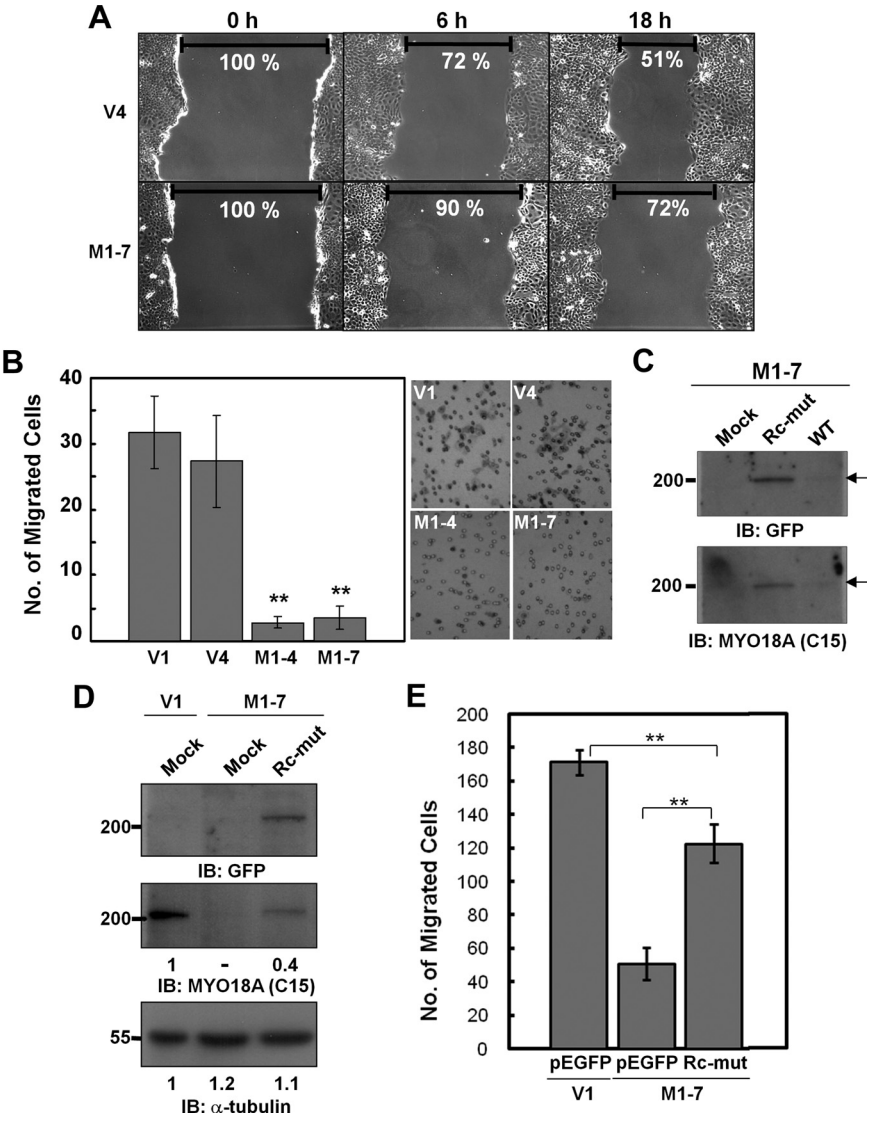

Figure 8. MYO18A is required for A431 cell migration. (A) Wound healing assay. Control and MYO18A-knockdown cells were cultured to confluence, scraped with a pipette tip, and photographed at the indicated time points. Data shown are representative of three independent experiments. (B) Transwell migration assay. Control and MYO18A-knockdown cells were harvested in serum-free medium and subjected to a transwell migration assay for 6 h using collagen I as a chemoattractant. The number of cells that had migrated to the bottom chamber was determined after staining with crystal violet. Values are the means ± SEs of the mean of data (n = 4 filters) from a representative experiment. **$p < 0.0005$ (two-tailed *t* test). Representative images of migrated cells from each of the four clones are shown in the right-hand panel. (C) M1-7 cells were transfected with vector (Mock), wild type (WT), or rescue mutant (Rc-mut) of pEGFP-C3/MYO18A for 48 h. Cells were then subjected to Western blot analysis using anti-GFP (top panel), or anti-MYO18A (C15) (bottom panel) antibodies. (D and E) Vector control V1 cells (transfected with pEGFP-C3 for 48 h) or M1-7 cells (transfected with pEGFP-C3 or Rc-mut of pEGFP-C3/MYO18A for 48 h) were collected for a 16-h transwell migration assay. *$p < 0.005$; **$p < 0.0005$ (two-tailed *t* test). Cells were then subjected to Western blot analysis using anti-GFP (top), anti-MYO18A (C15) (middle), or anti-tubulin (bottom) antibodies.

cluding the ER, membranes, cytosol, and nucleus (Brown *et al.*, 2002; Huang *et al.*, 2003), whereas MYO18A codistributes with actin fibers and locates to the inner surface of the cell membrane (Mori *et al.*, 2005; Isogawa *et al.*, 2005). It is notable that MYO18A was much more highly localized to ruffles versus lamellipodia (Figure 6 and Supplemental Figure S3). Our SEM data also revealed that membrane ruffles and dorsal filopodia were obviously vanished in the MYO18A-depleted cells (Figure 7C). Although the role of MYO18A in actin-myosin motor activity has not been fully elucidated, one possible explanation is that it is required in the contractile force needed for ruffle formation.

The third important finding of our work is the role of MYO18A in mediating the cellular distribution of the PAK2/βPIX/GIT1 complex. We observed that knockdown of MYO18A did not affect the formation of the PAK2/βPIX/GIT1 complex or the protein levels of its components, but did significantly increase the distribution of GIT1 and PAK2 to focal adhesions (Figures 5 and 7). PIX and the GITs have been shown to colocalize at focal complexes, the cell periphery and cytoplasmic complexes, suggesting that these proteins exist as oligomers at each of these sites (Turner *et al.*, 1999; Manabe *et al.*, 2002; Loo *et al.*, 2004). Because accumulation of GIT1 was observed in the focal contacts of MYO18A-depleted cells compared with control cells, the apparent localization of PAK2 to focal adhesions could be attributed to translocation of the PAK2/βPIX/GIT1 complex; however, as depletion of MYO18A could result in significant alterations of actin filaments and membrane ruffles in cells (Figure 7), the possibility that this phenomenon is resulted from an indirect effect of MYO18A depletion could not be excluded at present. Future work will be required to clarify this point. If our hypothesis is correct, the accumulation of PAK2/βPIX/GIT1 complexes might contribute to the increased number and enlarged size of focal adhesions, consequently leading to the enlarged morphology observed in MYO18A-knockdown cells. This could also partly explain why the MYO18A-depleted cells had significantly lower migration ability than control cells (Figure 8): an increased number of enlarged focal adhesions would be unfavorable to the rapid turn over of focal adhesions that is required for higher motility among motile cells (Lock *et al.*, 2008). Our live cell imaging data also support this explanation (Movies S1–S4).

Alteration of focal adhesions by manipulation of PAK has been reported in a variety of cell types, and numerous

reports have noted the accumulation of PAK, either active or inactive, in focal adhesions (for review, see Zegers, 2008). Although positive regulators that mediate the targeting of PAK to focal adhesions have been discovered, including NcK (Kiosses *et al.*, 1999; Zhao *et al.*, 2000) and PIX (Manser *et al.*, 1998; Zegers *et al.*, 2003), little is known about the negative regulator(s), if any, of this process. Because its discovery, MYO18A, an unconventional myosin with high molecular size and multiple domains, has been proposed to act as a scaffold protein (Furusawa *et al.*, 2000; Mori *et al.*, 2003). Our present findings that knockdown of MYO18A causes alteration of the subcellular locations of the PAK2/βPIX/GIT1 complex may provide a model to test this possibility in the future.

PAK2, when activated by the Cdc42 and Rac, was previously reported to catalyze phosphorylation and subsequent activation of intact nonmuscle MYO2, which may be physiologically important in regulating cytoskeletal organization (Chew *et al.*, 1998; Zeng *et al.*, 2000). MYO2A was reported to form a complex with MYO18A in murine alveolar monocytes (Yang *et al.*, 2005). Recently, MYO18A was reported by Leung's group to participate in the myotonic dystrophy kinase–related Cdc42-binding kinase (MRCK)/LRAP35a/MYO18A tripartite complex, which colocalizes extensively with lamellar actomyosin filaments in HeLa cells (Tan *et al.*, 2008). LRAP35a activates MRCK and targets it to actomyosin through the interaction with MYO18A, leading to regulatory myosin light-chain phosphorylation and MYO2A-dependent actomyosin assembly in the lamella. In addition, the promotion of persistent protrusive activity and inhibition of cell motility by the respective expression of wild-type and dominant-negative mutant components of the MRCK complex show that it plays a role in cell protrusion and migration (Tan *et al.*, 2008). In combination with the discovery of Leung's group that MYO18A is associated with a complex that is capable of modulating lamellar actomyosin retrograde flow, our present observation of an enlarged and flattened morphology for MYO18A-knockdown cells is perhaps unsurprising. Furthermore, both PAK2 and MRCK are downstream effectors of the small GTPase, Cdc42 (Manser *et al.*, 1994; Leung *et al.*, 1998). Thus, the findings from Leung's group and our present study demonstrate the specific role of MYO18A in cytoskeletal regulation and cell migration.

In conclusion, we herein demonstrate the existence of a previously unknown protein complex: PAK2/βPIX/GIT1/MYO18A. The regulatory role of MYO18A might account for some of the functions and molecular mechanisms of the PAK/PIX/GIT complex in actin filaments and focal contacts. Although our present findings shed new light on the functions of PIX/GIT complexes, numerous questions remain unanswered. For example, the role of small GTPases in regulating the complex formation and function is still a puzzle. What is the molecular mechanism of this complex in the turnover of actin filaments and focal adhesion, and in cell migration? Additional work, which is currently underway in our laboratory, will be required to fully understand the activity and biological impact of this novel interaction between MYO18A and PAK2.

ACKNOWLEDGMENTS

We thank the Kazusa DNA Research Institute (Chiba, Japan) for providing the KIAA0216 cDNA. We greatly appreciate Drs. Donna Webb, Edward Manser, and Peter L. Hordijk for kindly providing us the Paxillin-DsRed2, pXJ40-GST-GIT1, and pGEX-6P-bPIX plasmids, respectively. We also thank Confocal Microscopy Core Facility of Chang-Gung Memorial Hospital for technical assistance. This work was supported by grants from the National Science Council of Taiwan, Republic of China (NSC94-2745-B-182-003-URD, 95-2745-B-182-003-URD, 96-2320-B-182-031-MY3) and from Chang Gung University and Memorial Hospital, Taiwan, Republic of China (CMRPD140041 and 160041).

REFERENCES

Abo, A., Qu, J., Cammarano, M. S., Dan, C., Fritsch, A., Baud, V., Belisle, B., and Minden, A. (1998). PAK4, a novel effector for Cdc42Hs, is implicated in the reorganization of the actin cytoskeleton and in the formation of filopodia. EMBO J. *17*, 6527–6540.

Bagrodia, S., Taylor, S., Creasy, C., Chernoff, J., and Cerione, R. (1995). Identification of a mouse p21Cdc42/Rac activated kinase. J. Biol. Chem. *270*, 22731–22737.

Bagrodia, S., Bailey, D., Lenard, Z., Hart, M., Guan, J. L., and Premont, R. T. (1999). A tyrosine-phosphorylated protein that binds to an important regulatory region on the cool family of p21-activated kinase binding proteins. J. Biol. Chem. *274*, 22393–22400.

Berg, J. S., Powell, B. C., and Cheney, R. E. (2001). A millennial myosin census. Mol. Biol. Cell *12*, 780–794.

Beeser, A., Jaffer, Z. M., Hofmann, C., and Chernoff, J. (2005). Role of group A p21-activated kinases in activation of extracellular-regulated kinase by growth factors. J. Biol. Chem. *280*, 36609–36615.

Bokoch, G. M. (2003). Biology of the p21-activated kinases. Annu. Rev. Biochem. *72*, 743–781.

Brown, M. C., West, K. A., and Turner, C. E. (2002). Paxillin-dependent paxillin kinase linker and p21-activated kinase localization to focal adhesions involves a multistep activation pathway. Mol. Biol. Cell *13*, 1550–1565.

Chan, W. H., Yu, J. S., and Yang, S. D. (2000). Apoptotic signalling cascade in photosensitized human epidermal carcinoma A431 cells: involvement of singlet oxygen, c-Jun N-terminal kinase, caspase-3 and p21-activated kinase 2. Biochem. J. *351*, 221–232.

Chew, T. L., Masaracchia, R. A., Goeckeler, Z. M., and Wysolmerski, R. B. (1998). Phosphorylation of non-muscle myosin II regulatory light chain by p21-activated kinase (gamma-PAK). J. Muscle Res. Cell Motil. *19*, 839–854.

Coniglio, S. J., Zavarella, S., and Symons, M. H. (2008). Pak1 and Pak2 mediate tumor cell invasion through distinct signaling mechanisms. Mol. Cell. Biol. *28*, 4162–4172.

Cross, M., Csar, X. F., Wilson, N. J., Manes, G., Addona, T. A., Marks, D. C., Whitty, G. A., Ashman, K., and Hamilton, J. A. (2004). A novel 110kDa form of myosin XVIIIA (MysPDZ) is tyrosine phosphorylated following colony stimulating factor-1 receptor signaling. Biochem. J. *380*, 243–253.

Dan, C., Nath, N., Liberto, M., and Minden, A. (2002). PAK5, a new brain-specific kinase, promotes neurite outgrowth in N1E-115 cells. Mol. Cell. Biol. *22*, 567–577.

Feng, Q., Albeck, J. G., Cerione, R. A., and Yang, W. (2002). Regulation of the Cool/Pix Proteins. Key binding partners of the Cdc42/Rac targets the p21-activated kinases. J. Biol. Chem. *277*, 5644–5650.

Furusawa, T., Ikawa, S., Yanai, N., and Obinata, M. (2000). Isolation of a novel PDZ containing myosin from hematopoietic supportive bone marrow stromal cell lines. Biochem. Biophys. Res. Commun. *270*, 67–75.

Huang, Z., Ling, J., and Traugh, J. A. (2003). Localization of p21-activated protein kinase γ-PAK/Pak2 in the endoplasmic reticulum is required for induction of cytostasis. J. Biol. Chem. *278*, 13101–13109.

Hoefen, R. J., and Berk, B. C. (2006). The multifunctional GIT family of proteins. J. Cell Sci. *119*, 1469–1475.

Isogawa, Y., Kon, T., Inoue, T., Ohkura, R., Yamakawa, H., Ohara, O., and Sutoh, K. (2005). The N-terminal domain of MYO18A has an ATP-insensitive actin-binding site. Biochem. *44*, 6190–6196.

Jaffer, Z. M., and Chernoff, J. (2002). p21-activated kinases: three more join the Pak. Int. J. Biochem. Cell Biol. *34*, 713–717.

Kiosses, W. B., Daniels, R. H., Otey, C., Bokoch, G. M., and Schwartz, M. A. (1999). A role for p21-activated kinase in endothelial cell migration. J. Cell Biol. *147*, 831–844.

Knaus, U., Morris, S., Dong, H., Chernoff, J., and Bokoch, G. (1995). Regulation of human leukocyte p21-activated kinases through G protein–coupled receptors. Science *269*, 221–223.

Koh, C. G., Manser, E., Zhao, Z. S., Ng, C. P., and Lim, L. (2001). BetaPIX, the PAK-interacting exchange factor, requires localization via a coiled-coil region to promote microvillus-like structures and membrane ruffles. J. Cell Sci. *114*, 4239–4251.

Kumar, R., Gururaj, A. E., and Barnes, C. J. (2006). p21-activated kinases in cancer. Nat. Rev. Cancer *6*, 459–471.

Lee, N., MacDonald, H., Reinhard, C., Halenbeck, R., Roulston, A., Shi, T., and Williams, L. T. (1997). Activation of hPAK65 by caspase cleavage induces some of the morphological and biochemical changes of apoptosis. Proc. Natl. Acad. Sci. USA *94*, 13642–13647.

Lee, S. R., Ramos, S. M., Ko, A., Masiello, D., Swanson, K. D., Lu, M. L., and Balk, S. P. (2002). AR and ER interaction with a p21-activated kinase (PAK6). Mol. Endo. *16*, 85–99.

Leung, T., Chen, X. Q., Tan, I., Manser, E., and Lim, L. (1998). Myotonic dystrophy kinase-related Cdc42-binding kinase acts as a Cdc42 effector in promoting cytoskeletal reorganization. Mol. Cell. Biol. *18*, 130–140.

Lock, J. G., Wehrle-Haller, B., and Strömblad, S. (2008). Cell–matrix adhesion complexes: master control machinery of cell migration. Seminars Cancer Biol. *18*, 65–76.

Loo, T. H., Ng, Y. W., Lim, L., and Manser, E. (2004). GIT1 activates p21-activated kinase through a mechanism independent of p21 binding. Mol. Cell. Biol. *24*, 3849–3859.

Manabe, R., Kovalenko, M., Webb, D. J., and Horwitz, A. R. (2002). GIT1 functions in a motile, multi-molecular signaling complex that regulates protrusive activity and cell migration. J. Cell Sci. *115*, 1497–1510.

Manser, E., Leung, T., Salihuddin, H., Zhao, Z. S., and Lim, L. (1994). A brain serine/threonine protein kinase activated by Cdc42 and Rac1. Nature *367*, 40–46.

Manser, E., Loo, T. H., Koh, C. G., Zhao, Z. S., Chen, X. Q., Tan, L., Tan, I., Leung, T., and Lim, L. (1998). Pak kinases are directly coupled to the PIX family of nucleotide exchange factors. Mol. Cell *1*, 183–192.

Martin, G. A., Bollag, G., McCormick, F., and Abo, A. (1995). A novel serine kinase activated by rac1/CDC42Hs-dependent autophosphorylation is related to PAK65 and STE20. EMBO J *14*, 1970–1978.

Mori, K., Furusawa, T., Okubo, T., Inoue, T., Ikawa, S., Yanai, N., Mori, K. J., and Obinata, M. (2003). Genome structure and differential expression of two isoforms of a novel PDZ-containing myosin (MysPDZ) (Myo18A). J. Biochem. *133*, 405–413.

Mori, K., Matsuda, K., Furusawa, T., Kawata, M., Inoue, T., and Obinata, M. (2005). Subcellular localization and dynamics of MysPDZ (Myo18A) in live mammalian cells. Biochem. Biophys. Res. Commun. *326*, 491–498.

Obermeier, A., Ahmed, S., Manser, E., Yen, S. C., Hall, C., and Lim, L. (1998). Pak promotes morphological changes by acting upstream of Rac. EMBO J. *17*, 4328–4339.

Premont, R. T., Perry, S. J., Schmalzigaug, R., Roseman, J. T., Xing, Y., and Claing, A. (2004). The GIT/PIX complex: an oligomeric assembly of GIT family ARF GTPase-activating proteins and PIX family Rac1/Cdc42guanine nucleotide exchange factors. Cell Signal. *16*, 1001–1011.

Renkema, G. H., Manninen, A., and Saksela, K. (2001). Human immunodeficiency virus type 1 Nef selectively associates with a catalytically active subpopulation of p21-activated kinase 2 (PAK2) independently of PAK2 binding to Nck or beta-PIX. J. Virol. *75*, 2154–2160.

Royal, I., Lamarche-Vane, N., Lamorte, L., Kaibuchi, K., and Park, M. (2000). Activation of cdc42, rac, Pak, and rho-kinase in response to hepatocyte growth factor differentially regulates epithelial cell colony spreading and dissociation. Mol. Biol. Cell *11*, 1709–1725.

Rudel, T., and Bokoch, G. M. (1997). Membrane and morphological changes in apoptotic cells regulated by caspase-mediated activation of PAK2. Science *276*, 1571–1574.

Sells, M. A., Boyd, J. T., and Chernoff, J. (1999). p21-activated kinase 1 (Pak1) regulates cell motility in mammalian fibroblasts. J. Cell Biol. *145*, 837–849.

Tan, I., Yong, Dong, J., J. M., Lim, L., and Leung, T. (2008). A tripartite complex containing MRCK modulates lamellar actomyosin retrograde flow. Cell *135*, 123–136.

Tang, T. K., Chang, W. C., Chan, W. H., Yang, S. D., Ni, M. H., and Yu, J. S. (1998). Proteolytic cleavage and activation of PAK2 during UV irradiation-induced apoptosis in A431 cells. J. Cell. Biochem. *70*, 442–454.

Tsai, I. C., Hsieh, Y. J., Lyu, P. C., and Yu, J. S. (2005). Anti-phosphopeptide antibody, P-STM as a novel tool for detecting mitotic phosphoproteins: Identification of lamins A and C as two major targets. J. Cell. Biochem. *94*, 967–981.

Turner, C. E., Brown, M. C., Perrotta, J. A., Riedy, M. C., Nikolopoulos, S. N., and McDonald, A. R. (1999). Paxillin LD4 motif binds PAK and PIX through a novel 95-kD ankyrin repeat, ARF-GAP protein: a role in cytoskeletal remodeling. J. Cell Biol. *145*, 851–863.

Walter, B. N., Huang, Z., Jakobi, R., Tuazon, P. T., Alnemri, E. S., Litwack, G., and Traugh, J. A. (1998). Cleavage and activation of p21-activated protein kinase gamma-Pak by CPP32 (caspase 3). Effects of autophosphorylation on activity. J. Biol. Chem. *273*, 28733–28739.

Wu, C. C., Chien, K. Y., Tsang, N. M., Chang, K. P., Ho, S. P., Tsao, C. H., Chang, Y. S., and Yu, J. S. (2005). Cancer cell-secreted proteomes as a basis for searching potential tumor markers—nasopharyngeal carcinoma as a model. Proteomics *5*, 3173–3182.

Yang, C. H., *et al.* (2005). Identification of the surfactant protein A receptor 210 as the unconventional myosin 18A. J. Biol. Chem. *280*, 34447–34457.

Zegers, M. M., Forget, M. A., Chernoff, J., Mostov, K. E., ter Beest, M. B., and Hansen, S. H. (2003). Pak1 and PIX regulate contact inhibition during epithelial wound healing. EMBO J. *22*, 4155–4165.

Zegers, M. M. (2008). Roles of p21-activated kinases and associated proteins in epithelial wound healing. Int. Rev. Cell. Mol. Biol. *267*, 253–298.

Zeng, Q., Lagunoff, D., Masaracchia, R., Goeckeler, Z., Cote, G., and Wysolmerski, R. (2000). Endothelial cell retraction is induced by PAK2 monophosphorylation of myosin II. J. Cell Sci. *113*, 471–482.

Zhao, Z. S., Manser, E., Loo, T. H., and Lim, L. (2000). Coupling of Pak-interacting exchange factor PIX to GIT1 promotes focal complex disassembly. Mol. Cell. Biol. *20*, 6354–6363.